# The Development of a Genetically Encoded Tool to Inquire into Organelle Morphology

**By**
**Elmer Rho**

A thesis submitted to Johns Hopkins University in conformity with the requirements for the degree of Master of Science in Biomedical Engineering

**Baltimore, Maryland**
**May 2017**

# Abstract

Organelles take various forms of shapes and sizes. Alteration to its structure allows organelles to either carry out unique tasks or to adapt to the ever-changing cellular environment. For example, the reticular nature of the peripheral endoplasmic reticulum is important for the passage of macromolecules from the cytosol to the plasma membrane whereas fragmented forms of mitochondria ensure proper segregation to the daughter cells during mitosis [1,2,3]. Another example will be mitochondria forming donut shaped structures after hypoxia-reoxygenation [4]. Thus, the morphology of organelles plays an active role in countless critical cellular processes, and therefore, it is not surprising for researchers to study the relation between morphology and different disease states.

To date, it is clear what consequences each type of morphology is associated with; however, it is yet to be determined whether the morphology itself can bring about certain ramifications. This results from the limitations in tools to dissociate the role of morphology from the complex signaling network. As a result, a natural question will be whether it is possible to develop a tool that can directly manipulate organelle morphology so that it is possible to inquire into the effects of perturbed organelle morphology in a stepwise manner.

This paper will focus particularly on mitochondrial morphology and introduce the biochemistry of mitochondrial dynamics, diseases associated with impaired mitochondrial morphology, and current tools to unravel mitochondrial physiology.

Lastly, the paper will survey a novel tool that could potentially be used to dissect the role of mitochondrial morphology through direct manipulation of its morphology which will be the first tool to exploit actin-based forces to achieve this.

**Advisor:** Dr. Takanari Inoue

**Readers:** Dr. Takanari Inoue; Dr. Rebecca Schulman; Dr. Kevin Yarema

# Acknowledgements

I would like to thank Dr. Takanari Inoue, Hideki Nakamura, and all members of the Inoue lab for their support, guidance, and constructive criticism throughout my two years of my thesis project. I would also like to thank all the undergraduates Albert Yang, Brian Huang, and Zi-Yi Choo for their enormous help on the project. I truly believe whatever achievements I made throughout my career would not have happened without everyone's kindness and assistance. I would also want to say thank you to my family for their overflowing love and encouragement. Finally, I thank the BME Master's Program for the incredible research experience!

# Table of Contents

# List of Tables

# List of Figures

# Mitochondrial Dynamics and Current Tools

## 1. Mitochondria Dynamics

Mitochondria morphology is dynamically shaped through the balance of fusion and fission. Fusion is the process where two organelles come together to become a single identity. It is an intricate and delicate procedure where multiple proteins are involved to rupture, deform, and merge the lipid bilayers. Fusion starts off by joining the outer membranes together under the coordination of dynamin-like GTPases such as mitofusins 1 and 2 (Mfn1 and Mfn2) [3,4,5,6,7]. Mfns contain a conserved GTPase domain and coiled-coil structure at its carboxyl-tail, and they mediate outer-membrane fusion through homo- and heterotypic interactions at the expense of GTP [5,7]. This causes a conformational change allowing to membrane structure to fuse together (Fig 1.1). Inner membrane fusion occurs in a similar fashion but instead requires a GTPase called Opa1 (Fig 1.1) [7,8]. The coordination between inner and outer membrane fusion is yet to be understood, but current belief is that the two events work together through an adaptor protein which somehow links the two inner and outer membrane fusion proteins and allowing information exchange.

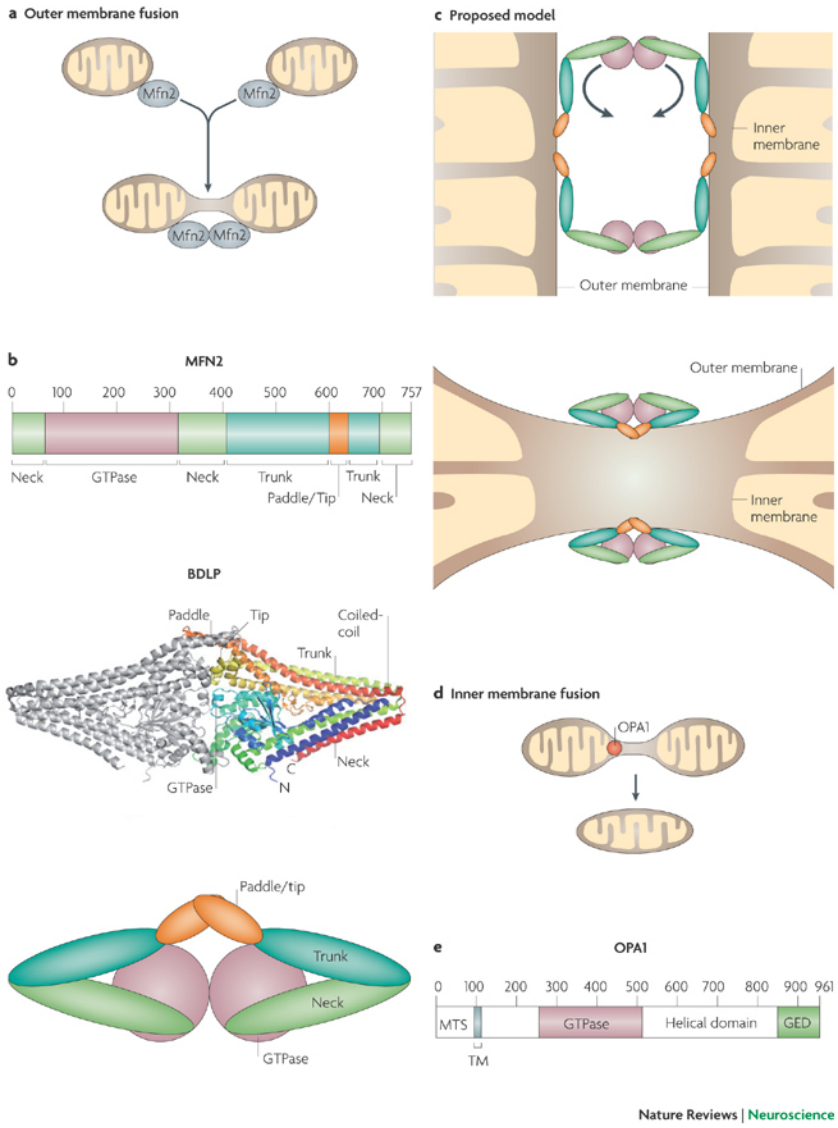


**Figure 1.1: Mechanism of Mitochondrial Fusion.** A schematic of mitochondrial outer (Mfn2) and inner membrane fusion proteins (Opa1). (Adapted from A. B. Knott and G. Perkins, Nature Reviews Neuroscience 2008)

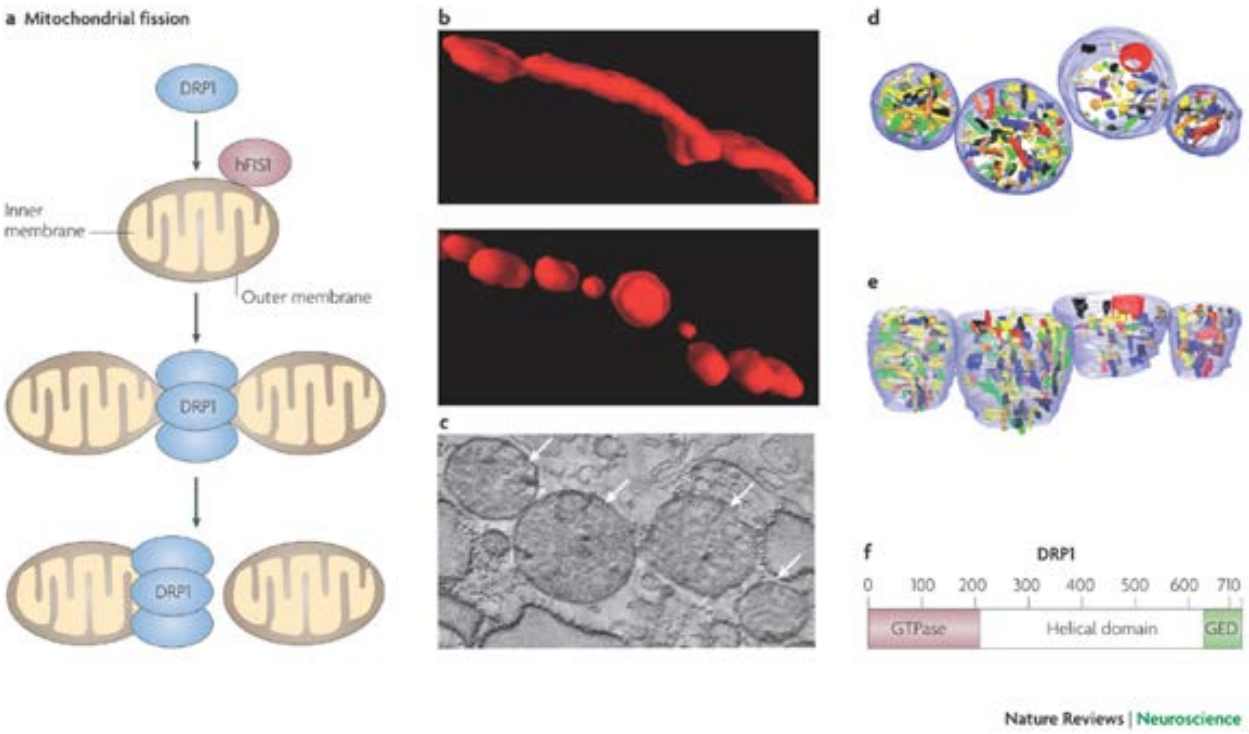


**Figure 1.2: Mechanism of Mitochondrial Fission.** An illustration of mitochondrial fission protein, Drp1, involved in mitochondrial fragmentation (Adapted from A. B. Knott and G. Perkins, Nature Reviews Neuroscience 2008)

Mitochondrial fission involves a dynamin-related protein, Drp1 [9]. One unique property of Drp1 is that majority of Drp1 remains cytosolic but can self-assemble on the mitochondrial membrane and subsequently induce GTP hydrolysis to generate a constriction force (Fig 1.2) [7,9,10]. Recent reports postulate that actin filaments may accelerate Drp1 oligomerization at the membrane by promoting its interaction with receptors such as mitochondrial fission factor (MFF) [10,11]. On the mitochondrial membrane, Drp1 forms a spiral-helix, and upon GTP hydrolysis, the helices rotate relative to each other promoting constriction [7,9,10,11].

# 2. Disruption of Mitochondrial Morphology and Diseases

So why is mitochondrial dynamics important? It has been reported that mitochondrial fusion is imperative for maximizing ATP production and facilitating content exchange [5,6,**7,**12]. This

serves as a protective mechanism for individual mitochondria that would otherwise be susceptible to damage. On the other hand, mitochondrial fission is vital for segregating damaged mitochondria from healthy pool of mitochondria for elimination [13], and has been typically linked with apoptosis [14,15]. Mitochondrial fission is also important in cell division to equally distribute mitochondria to daughter cells [16]. Thus, mitochondrial dynamics takes a large part in maintaining cellular integrity, energy production, calcium regulation, and cell division. Therefore, it is unsurprising that defects in mitochondrial dynamics is associated with many devastating diseases such as neuronal and myocardial diseases.

Due to the large energy demand, numerous neuronal processes rely on mitochondrial dynamics and neurodegenerative diseases arise as a consequence of deficiency in mitochondrial fusion and fission proteins. In particular, mutations in the Mfn2 gene leads to diseases such as Charcot-Marie-Tooth disease (CMT), a peripheral neuropathy that is characterized by muscle weakness and axonal degradation of sensory and motor neurons., hereditary motor and sensory neuropathy which results in optic atrophy and visual impairments [17,18]. Mutations in Opa1 cause a more common optic atrophy, autosomal dominant optic atrophy (ADOA) [6,17,18].

Heart failures are another common disorder resulting from impairment in mitochondrial morphology. Recent studies by Thomas Langer have shown that the dysregulation of mitochondrial morphology leads to changes in metabolic status, a shift from fatty acid oxidation to glucose utilization, in cardiomyocytes and this precedes heart failure [19]. It has been shown that the L-Opa1 mediated mitochondrial fusion preserves cardiac function whereas proteolytic processing of L-Opa1 to S-Opa1 by a mitochondrial protease, OMA1, triggers dilated cardiomyopathy and heart failure [19].

# 3. Tools to Understand Mitochondrial Dynamics and Limitations

As much as mitochondrial dynamics is important, to date, various methods and tools to study mitochondrial function have been developed. These tools range from dyes and drugs to genetically encoded proteins that can either measure various parameters of the mitochondria such as membrane potential, ATP levels, calcium levels, etc. or tools such as CCCP and knock out models to perturb the mitochondrial integrity to understand the effects of morphological and functional defects [20]. Although many of these tools have broaden our understanding of the field of mitochondrial dynamics, they are still far from being perfect.

Carbonyl cyanide *m*-chlorophenyl hydrazine (CCCP) is a chemical drug that has been widely used to understand mitochondrial functionality rather than morphological studies. It decreases mitochondrial membrane potential by binding to protons in the intermembrane space and transferring into the matrix [21]. The uncoupling of proton gradient induces a pathway that leads to activation of various processes that causes mitochondrial fragmentation and degradation. Therefore, because of its acute effects on the membrane potential, it is typically used in studying mitophagy and consequences of impaired mitochondria [22,23,24].

Several small molecules to study mitochondrial dynamics has been reported. Dynasore is a small molecule that inhibits the GTPase activity of dynamin. It noncompetitively binds to the GTPase domain of all dynamins in both assembled and unassembled states [25,26]. However, one issue is that it is unspecific and inhibits all dynamins (dynamin1, dynamin2, and Drp1) [25,26]. GTPγs, a non-hydrolyzable GTP, is another method to inhibit Drp1, but once again antagonizes all GTPases [27]. To address the limitations of current inhibitors, a novel inhibitor, Mdivi-1, has been developed. It is postulated that Mdivi-1 selectively binds to an allosteric site of mitochondrial

division Drp1 that does not act through the GTPase domain. Upon Mdivi-1 binding, it is speculated that Drp1 is locked into an unassembled form which cannot assemble into Drp1 filaments/spirals; however, there is no convincing evidence such is the case [27,28,29]. In addition, recent report suggests that Mdivi-1 is more of a mitochondrial complex 1 inhibitor rather than Drp1 inhibitor [30]. They've shown that there are discrepancies in phenotypes between Drp1 KO cells and Mdivi-1 cells and attributed the effects of Mdivi-1 to Drp1-independent mechanisms such as regulation of mitochondrial fusion proteins [31]. Despite the fact these drugs circumvent the need for generating mutant or knockout models and provide an opportunity to take discrete steps to understand mitochondrial dynamics rapidly, there is still an imperfect understanding of the mechanism and the extent of these approaches [30].

In the case of knock out models, they have their own set of limitations when used to study mitochondrial morphology. One example is knocking out fusion/fission proteins or overexpressing its counterpart leads to different functional changes in the mitochondria. For example, deletion of Mfn2 in skeletal muscle causes mitochondrial fragmentation which ruins the metabolic signaling of these tissues. On the contrary, overexpression of Drp1 does not cause mitochondrial fragmentation but results in increased mitochondrial length. In case of the liver, deletion of Drp1 induces mitochondrial fragmentation [6]. Thus, deletion of the same protein can result in different morphological phenotypes across different tissues. Furthermore, mitochondria of cardiac cells in Mfn1 KO mice showed larger mitochondria whereas in Mfn2 KO cells, the mitochondria were fragmented implying that deletion of genes that have similar roles in mitochondrial morphology doesn't necessarily lead to identical phenotypes and complicating the issue [31]. These observations suggest the need for a consistent and comprehensive method to assess mitochondrial morphology.

# Developing Actin Based Tool for Mitochondrial Morphology Studies

## 1. Background in Actin Polymerization

Actin polymerization is one of the most universally employed mechanism to generate force in living cells such as endocytosis [34], cell migration [35], vesicle trafficking [36], and cytokinesis [37]. There are various types of actin polymerization each initiated through a unique mechanism producing different forms of actin polymerization for different purposes. One is formin induced actin polymerization which creates unbranched actin filaments [38,40]. Another is spire proteins which initiates actin polymerization via WASP-homology 2 (WH2) domains [39,40]. Finally, there is Arp2/3 dependent actin polymerization which promotes actin polymerization by mimicking an actin dimer or trimer to provide a scaffold for successive actin filament binding [40]. Arp2/3 dependent actin polymerization, in particular, requires the activity of nucleation promoting factors (NPFs). Some examples of NPFs are WASP, SCAR, and WAVE. Rho-family GTPases CDC42 and Rac activates the auto-inhibited NPFs which subsequently initiates actin polymerization by binding to Arp2/3 through its acidic domain [40]. The central region induces

conformational change of Arp2/3 and together with other domains delivers free actin polymers to the barbed ends of growing actin filaments and ATP hydrolysis reduces Arp2 interaction with mother filament preparing for additional branching or setting the onset of debranching.

# 2. ActA from *Listeria Monocytogenes*

*Listeria Monocytogenes* is a foodborne pathogen that causes listeriosis, a disease characterized by severe gastroenteritis, encephalitis, meningitis or septicemia, as well as miscarriage [41-45]. One of the fascinating features of *Listeria* is that it swims through the host cytoplasm by producing an actin comet tail. This is achieved through a protein called ActA which is asymmetrically distributed along the surface of *Listeria* through its transmembrane domain [41-43]. This asymmetry along with having its various domains that trigger actin polymerization facing towards the host cytoplasm allows it to highjack the host actin machinery to form a self-propelling actin cloud. [44,45] That being said, ActA is sufficient to drive *Listeria* motility.

So what is this protein called ActA? Through systematic domain analysis, it has been revealed that ActA is divided into domains that are similar to NPFs such as the proteins in the WASP family [41,46]. These domains include the signaling peptide, acidic domain, actin-monomer binding domain, cofilin-homology domain, proline-rich domain, and transmembrane domain. The acidic domain, actin-monomer binding domain, and cofiilin homology domain together constitute the minimal component required for actin polymerization and hence, *Listeria* motility [41,46]. It mimics the Verprolin-Cofilin-Acidic (VCA) domain of the WASP family. One key difference is that unlike the proteins of the WASP family, its activation is not dependent on Cdc42 and is in a constitutively active form.

The ability of ActA to bind to and activate Arp2/3 complex is achieved by the cofilin-homology domain and the efficiency and the rate of actin polymerization is accomplished through the acidic

domain [42,43]. The proline rich domain contains four proline repeats which bind to Ena-VASP proteins by mimicking host cell cytoskeletal proteins such as zyxin, vinculin, and paladin [42]. Subsequent biochemical studies have shown that ActA has a higher affinity towards these Ena-VASP proteins than the host cell cytoskeletal proteins [42,47]. Although these proteins are not required for *Listeria* motility, they increase the speed and directional persistence [47].

# 3. ActA as a Tool?

One of the first demonstration of ActA as force generator was shown *in vitro* bead studies where they've shown ActA alone is sufficient to stimulate Arp2/3 complex and initiate actin polymerization and generates actin comet tails [49-53]. Further examples of ActA as a molecular force generator include expressing ActA in *S. Pneuoniae* and coating synthetic liposomes to provide actin-based motility.

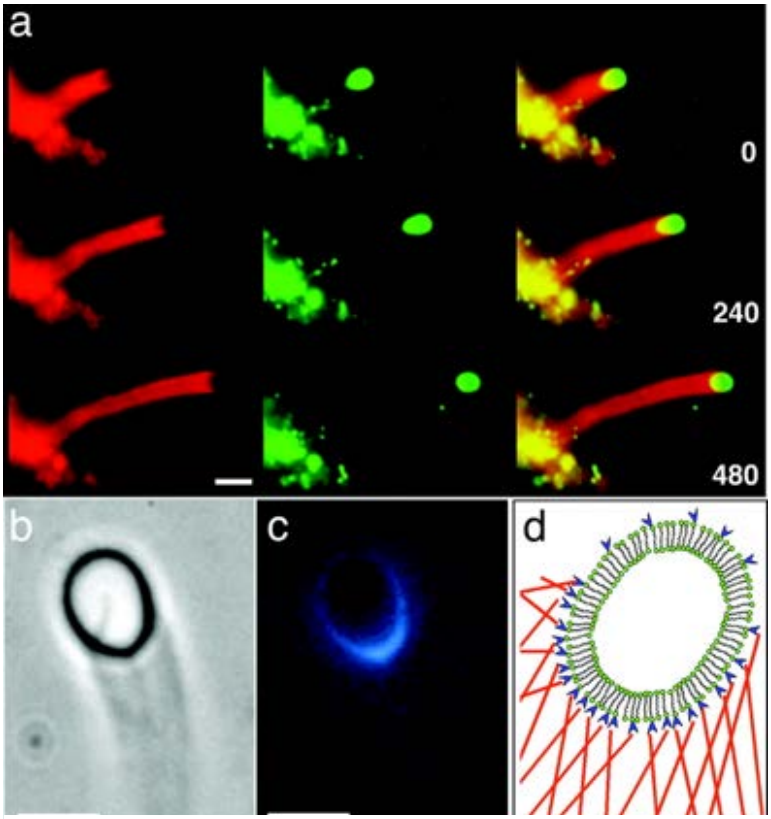


**Figure 2.1: Actin driven motility of ActA coated lipid vesicles**. Vesicles were labeled with Oregon Green, and actin was labeled with rhodamine. (Adapted from *Arpita Upadhyaya et al. PNAS*, 2004**)**

Some studies suggested that force generation is done through the addition of actin monomer between the space between the growing actin filaments and the membrane. The actin filament transiently binds and dissociates from the membrane and during this process actin monomers come into this gap pushing the membrane. The process is repeated

until the actin filaments are capped and prevented from re-associating with the membrane. However, the overall biophysical mechanism by which each actin filaments cooperatively execute such dramatic behavior is yet to be resolved.

The large magnitude of force it generates is implicated in the high speed at which *Listeria* moves. It has been reported that in Xenopus frog egg cytoplasmic extracts, *Listeria* moves approximately 100nm/s on average [49,50]. One group estimated the force generated by ActA using synthetic liposomes where they approximated the force to be around 3000pN/$\mu m^2$ which was comparable to lamellipodia stall forces, 2000pN/$\mu m^2$ [51]. That being said, it is imaginable to use ActA as a tool to deform membranes. Evaluation of ActA as a tool was conducted through the following five major experiments.

# Experiment 1

## 1.1 Codon Optimization and Characterization of Overexpressed ActA

To date, expression of ActA in mammalian cells have not been reported; therefore, it is crucial to know how well this bacterial protein is expressed in mammalian cells and its effects on organelle morphology. We took the ActA gene and transferred it to a plasmid driven by mammalian expression promoter (CMV-promoter).

Full length ActA was expressed in Hela cells; however, as shown in Fig 3.1, the expression was too low to carry out any meaningful experiment. We assumed this was due to the different codon usage between mammalian and bacterial cells, and therefore, we codon optimized ActA for mammalian expression (mActA) and as shown in Fig 3.1 (a), the expression improved.

To assess the localization of mActA, we expressed mActA with either an endoplasmic reticulum (ER) marker (KDEL) or a mitochondria marker (Tom20) and a marker for F-actin (Lifeact). We found out that compared to the control cells, which did not have mActA expressed, the ER morphology was abnormally crowded around the periphery of the

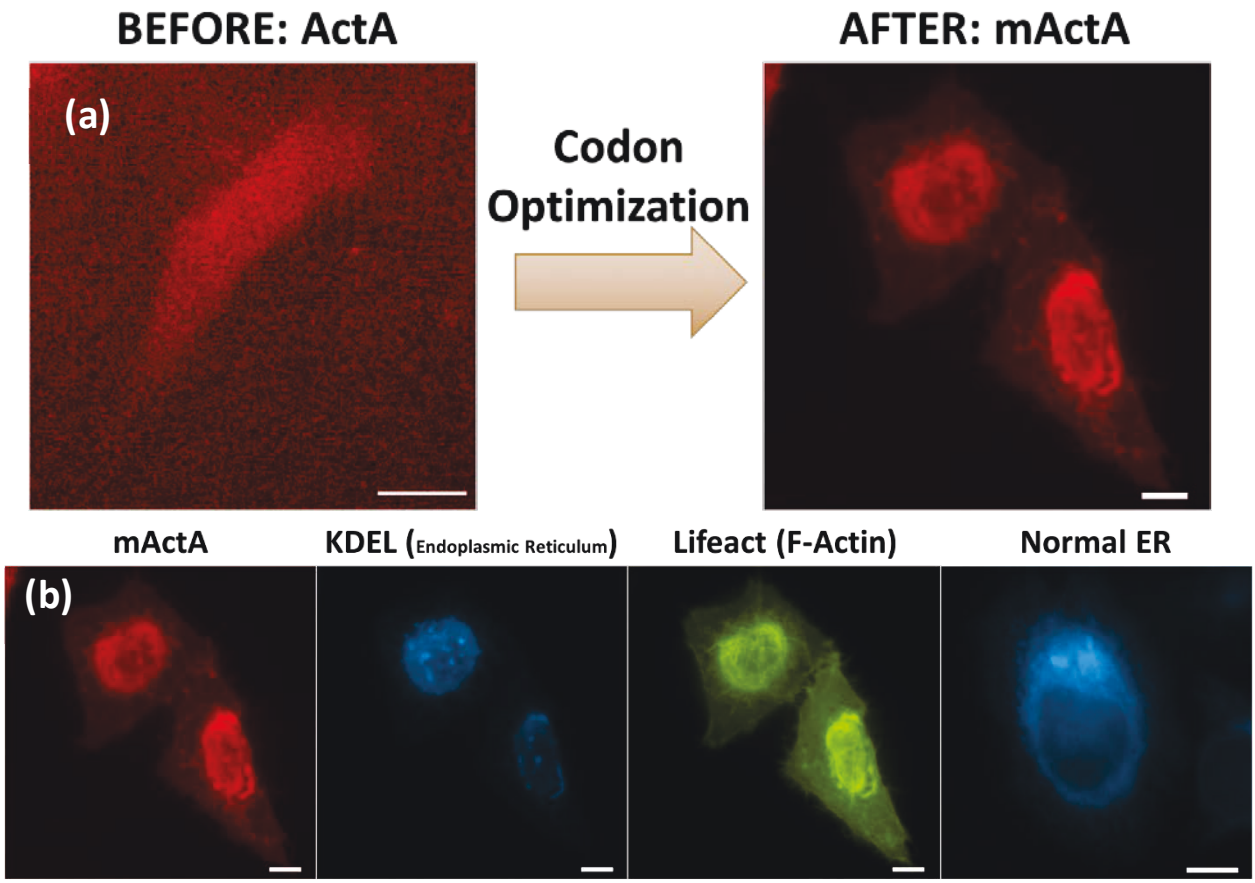


**Figure 3.1: Comparing the expression and localization of non-codon optimized ActA and codon optimized ActA, mActA.** (a) Codon optimized ActA has higher level of expression compared to the non-codon optimized one. (b) codon=optimized ActA co-expressed with **an** endoplasmic reticulum (ER) marker and a F-actin marker, LIfeact. Compared to the normal ER, the morphology of the ER in cells with mActA has a very deformed structure with increased accumulation of F-actin.

nucleus with high level of mActA and F-actin signal around the deformed ER suggesting that F-actin accumulation could be involved in this atypical appearance of the ER (Fig 3.1 (b)).

# 1.2 Engineering a diffusive mActA

ActA is divided into several domains: signaling peptide sequence acidic domain, actin monomer binding domain, proline rich regions, and transmembrane domain. We hypothesized that the reason why we see mActA localized at the ER is because of its transmembrane domain. Therefore, to dissociate mActA from the ER and have it relocated to the cytosol, we removed the transmembrane

domain and signaling peptide region of mActA and named this truncated version as $mActA_{diff}$. We again coexpressed $mActA_{diff}$ with an ER marker (KDEL), mitochondria marker (Tom20), and a F-actin marker (Lifeact), and as expected, $mActA_{diff}$ was now uniformly localized throughout the cell and the morphology of both mitochondria and ER looked normal as characterized by its highly networked and tubular structure. In addition, F-actin signal was high at the cytosol relative to the control. This was further confirmed with phalloidin staining.

# Experiment 2

## 2.1 mActA$_{diff}$ to Perturb Organelle Morphology

Based on what we've observed with the full length ActA, we hypothesized that accumulation of mActA$_{diff}$ at a subcellular structure could mechanically deform the it through actin polymerization. To test this idea, we took advantage of a method called chemically-inducible-dimerization (CID) in which two proteins FRB and FKBP dimerizes upon addition of a chemical called rapamycin [54].

Either FRB or FKBP was fused to the C-terminus of mActA$_{diff}$ and the other pair was fused to the outer membrane of the target organelle (Fig 3.2). We targeted mActA$_{diff}$ to the outer membrane of the mitochondria, and seconds after translocating mActA$_{diff}$, the mitochondria tubules broke down into small circular like vesicles with high F-actin signal around the mitochondria as indicated by the Lifeact signal (Fig 3.3).

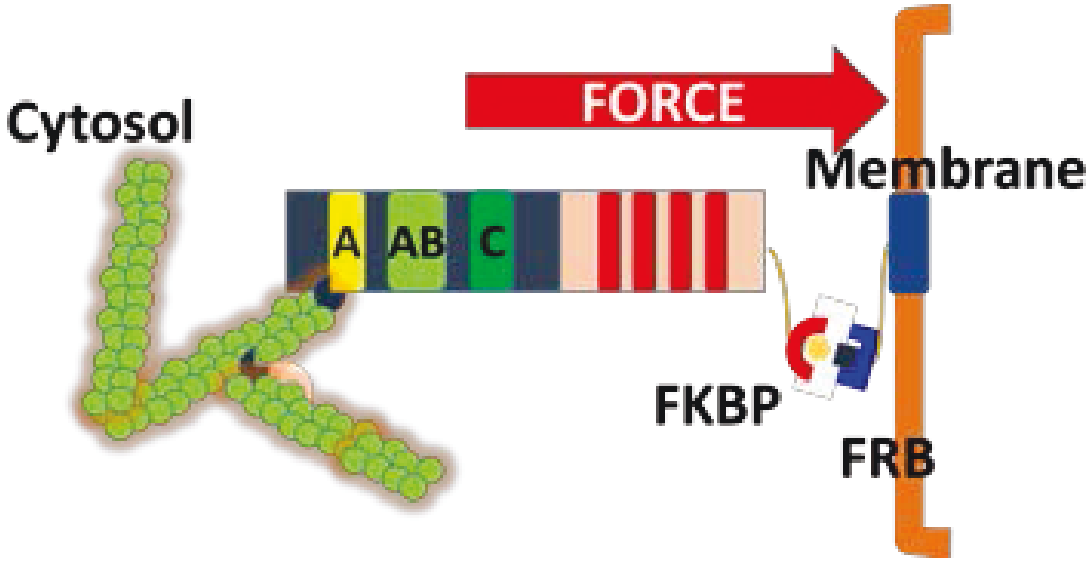


**Figure 3.2: Illustration of using mActA$_{diff}$ to generate force on organelle membrane.** Either FKBP or FRB was fused to the C-terminal of mActA$_{diff}$ or an organelle-targeting sequence. This would generate force at the targeted organelle membrane through actin polymerization.

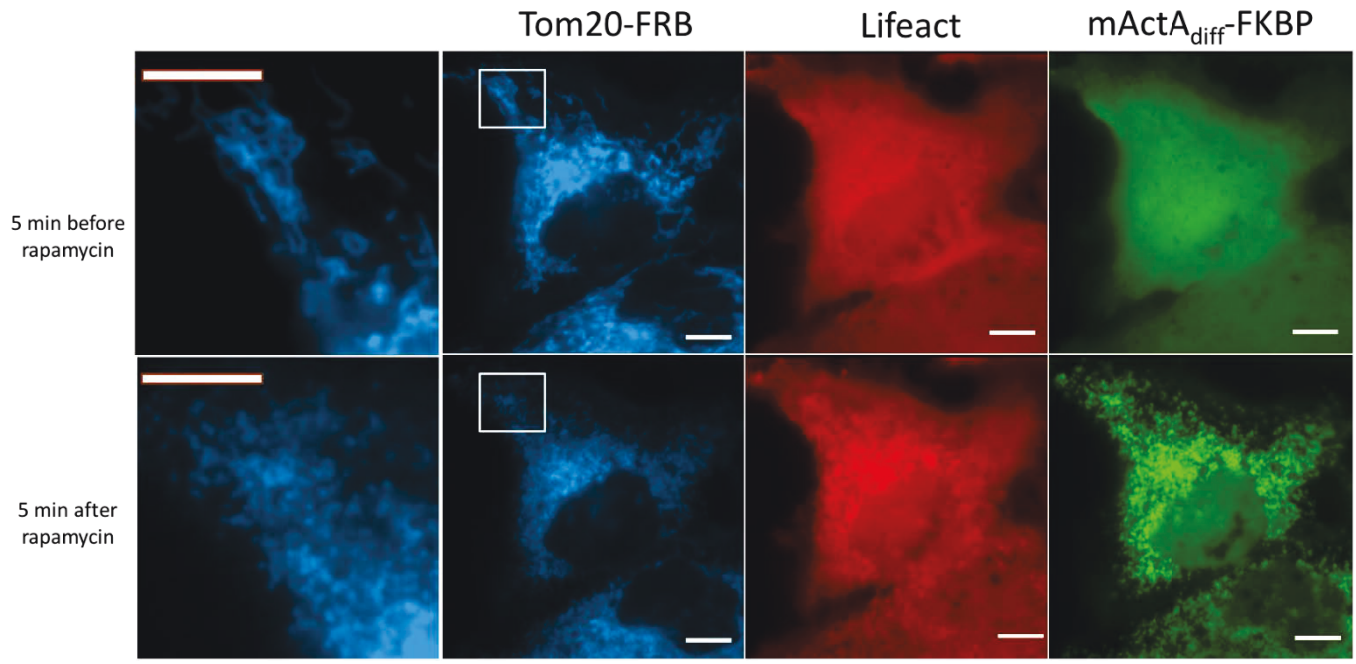


**Figure 3.3: mActA$_{diff}$ targeted to the outer membrane of the mitochondria.** mActA$_{diff}$ and TOM20 was fused to either FRB and FKBP. Upon addition of rapamycin, mActA$_{diff}$ translocated to the mitochondria. As soon as it was translocated, high accumulation of F-actin was observed and the mitochondria tubules were broken down to tiny fragments.

## 2.2 Comparing with other Actin Nucleators

We then asked whether this phenotype could be observed with other various actin nucleators. N-WASP, VCA domain of NWASP (deltaN-NWASP), SH3-domain of NCK, and Espfu5R were targeted to the mitochondria using CID. Upon recruitment of each of these actin nucleators, we either did not see mitochondrial fragmentation or the process was very slow. This shows that $mActA_{diff}$ is the best candidate in terms of mitochondrial fragmentation (Fig 3.4).

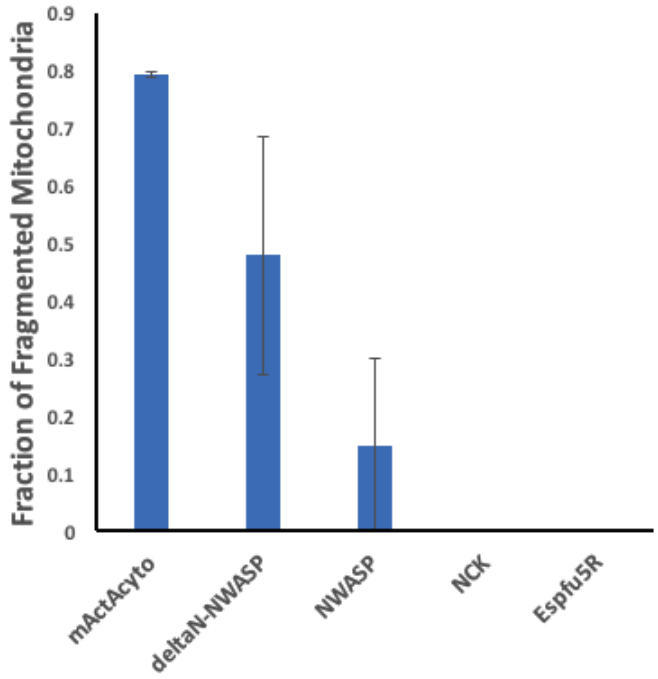


**Figure 3.4: $mActA_{diff}$ is the best candidate for deforming mitochondrial morphology.** deltaN-NWASP (constitutively active N-WASP), N-WASP, SH3 domain of NCK, and Espfu5R (a pathogenic protein) were targeted to the outer membrane of the mitochondria. The fraction of fragmented mitochondria was calculated by counting the number of cells that visually showed fragmented mitochondria and dividing by the total number of cells that showed translocation.

To examine whether the entire domain structure of $mActA_{diff}$ is required for its full ability to fragment the mitochondria, we split $mActA_{diff}$ into two pieces by its domain, mActA(1-235) and mActA(235-584). mActA(1-234) comprised the acidic region (A), actin monomer binding region

(AB), and cofilin region (C) while mActA(235-584) contained the proline rich region. Each of these proteins were translocated to the mitochondria, and we found out that the effects on the mitochondria decreased compared to $mActA_{diff}$. The overall kinetics were slower. This leads to a conclusion that the overall structure of $mActA_{diff}$ is important for mitochondrial fragmentation. This was further confirmed by measuring the fluorescence of the phalloidin staining in the cytosol. The fluorescence signal was greatest in $mActA_{diff}$ indicating that full structure is required for maximum actin polymerization activity (Fig 3.5).

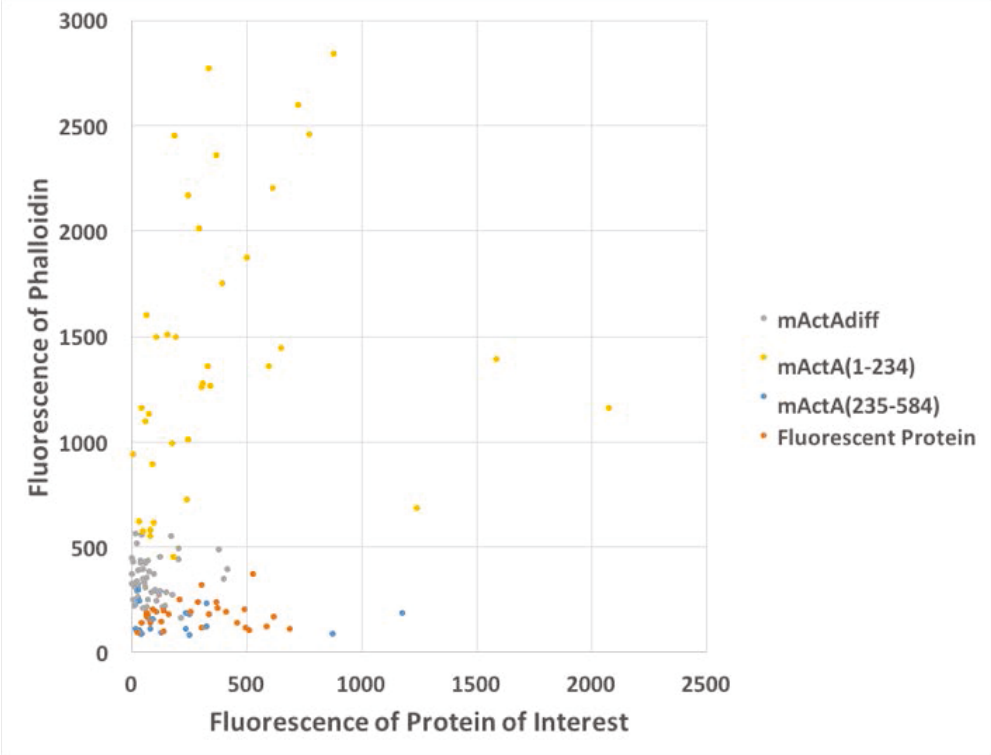


**Figure 3.5: Phalloidin staining reveals overall structure of $mActA_{diff}$ is essential for actin polymerization.** $mActA_{diff}$, mActA(1-234), mActA(235-584), and fluorescent protein were individually expressed in cells, and the cells were stained with phalloidin. The level of staining was quantified by measuring the fluorescence intensity and was used as a readout for background actin polymerization activity. The fluorescence of each protein was used as a readout for the expression level of the protein. $mActA_{diff}$ had the highest phalloidin staining per expression.

# Experiment 3

## 3.1 Characterizing the Mechanism of $mActA_{diff}$ Induced Mitochondrial Fragmentation

We further sought to determine whether the fragmentation was due to actin polymerization. To test this, we pretreated cells with Latrunculin A, which inhibits actin polymerization by sequestering free G-actin. After pretreating cells, $mActA_{diff}$ was targeted to the outer membrane of the mitochondria. As shown in Fig 3.7, there was no visible mitochondrial fragmentation and no accumulation of F-actin at the mitochondria. Furthermore, we co-expressed Arp2, and after recruitment of $mActA_{diff}$, we saw an acute accumulation of Arp2 indicating that Arp2/3 was involved (Fig 3.6).

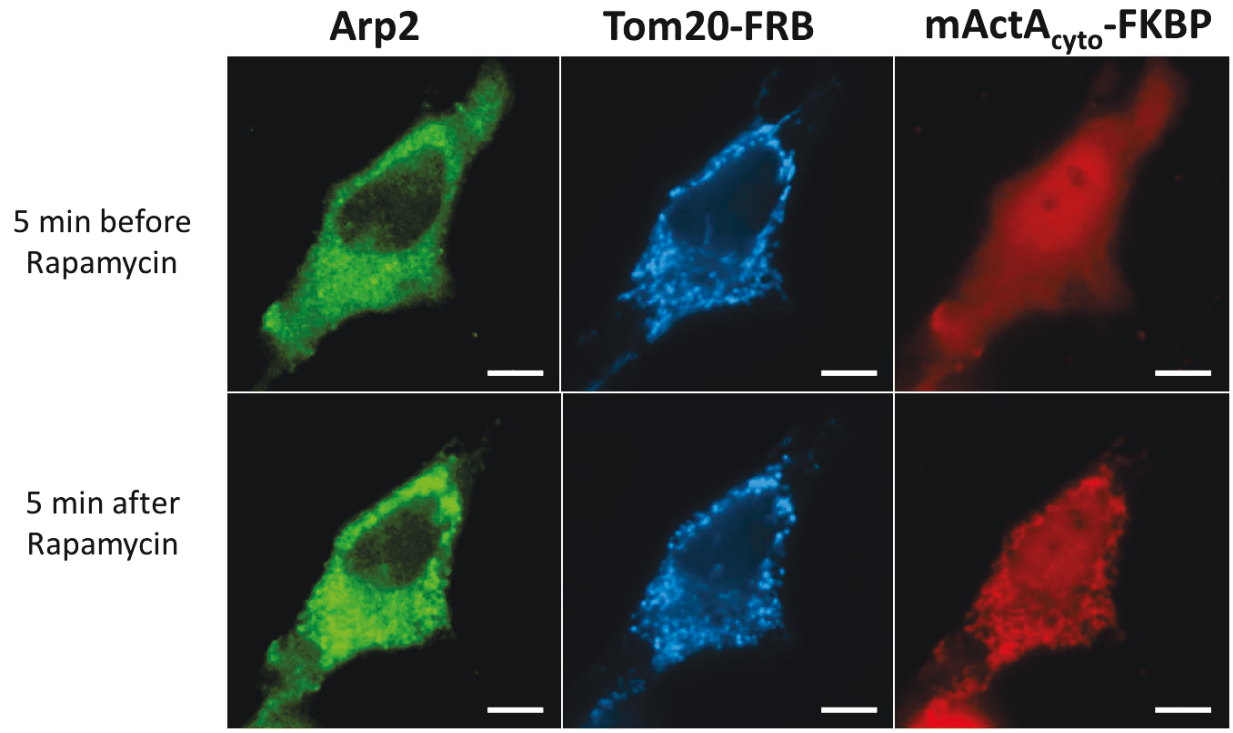


**Figure 3.6: mActA$_{diff}$ induced mitochondrial fragmentation involves the Arp2/3 complex.** mActA$_{diff}$ and TOM20 was fused to either FRB and FKBP and co-expressed with Arp2. Upon addition of rapamycin, mActA$_{diff}$ translocated to the mitochondria and Arp2 was recruited to the mitochondrial fragment sites.

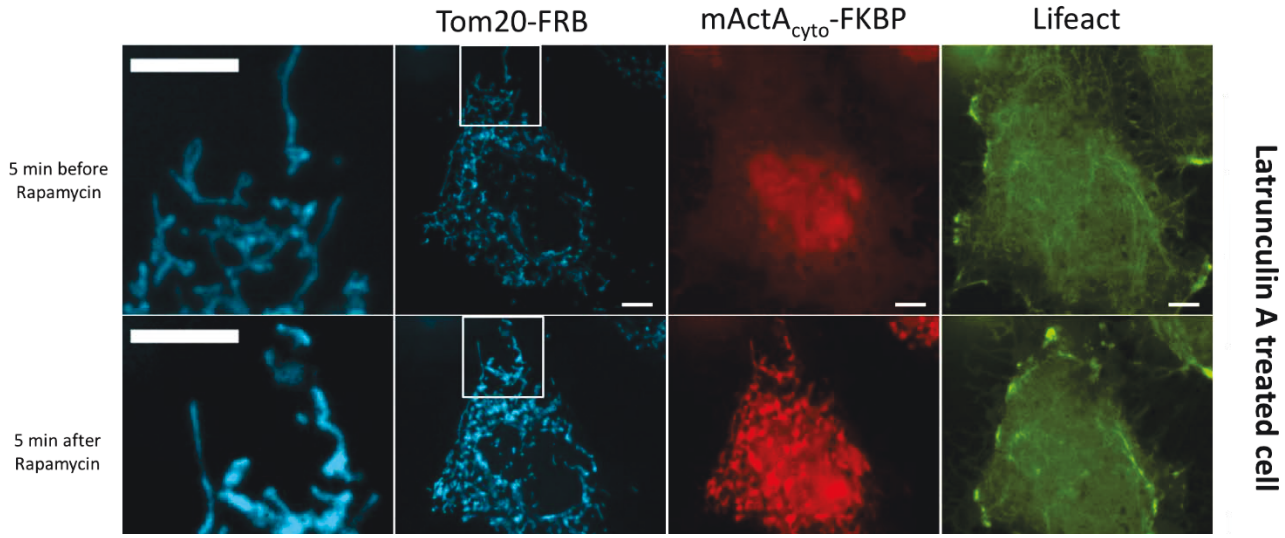


**Figure 3.7: mActA$_{diff}$ induced mitochondrial fragmentation is dependent on actin polymerization.** mActA$_{diff}$ and TOM20 was fused to either FRB and FKBP. Hela cells were pretreated with 500nM Latrunculin A. Upon addition of rapamycin, mActA$_{diff}$ translocated to the mitochondria. The mitochondria did not fragment and F-actin accumulation was not observed.

Next, we wanted to see whether the fragmentation was independent of myosin II. We pretreated cells with blebbistatin which blocks myosin II activity, and upon recruitment of $mActA_{diff}$ to the mitochondria, the mitochondria fragmented indicating that the fragmentation was independent of myosin II (Fig 3.8).

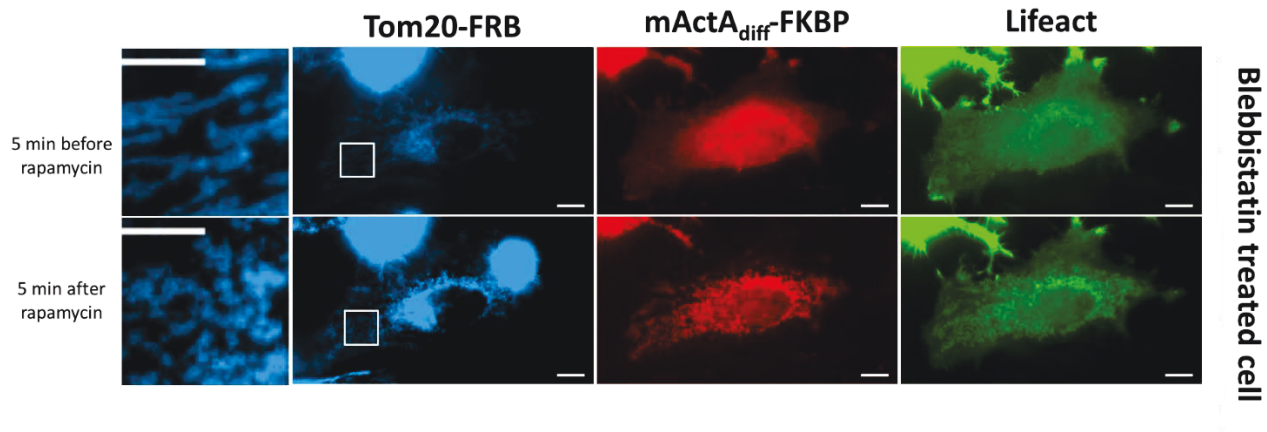


**Figure 3.8: $mActA_{diff}$ induced mitochondrial fragmentation is independent of actin polymerization.** $mActA_{diff}$ and TOM20 was fused to either FRB and FKBP. Hela cells were pretreated with 50uM of blebbistatin for 30min. $mActA_{diff}$ caused mitochondrial fragmentation upon recruitment to the mitochondria.

To exclude the possibility that $mActA_{diff}$ exploits endogenous mitochondrial fission machinery, we attempted to fragment the mitochondria in Drp1 KO MEFs. Surprisingly, it took more time (~20 min) for the mitochondria in Drp1 KO MEFs to fragment (Fig 3.9). This could be due to the long mitochondria of Drp1 KO MEFs or another possible explanation could be that endogenous fission machinery facilitates $mActA_{diff}$ induced fragmentation which was absent in Drp1 KO MEFs. Regardless, this result indeed suggests that the fragmentation induced by $mActA_{diff}$ is Drp1 independent.

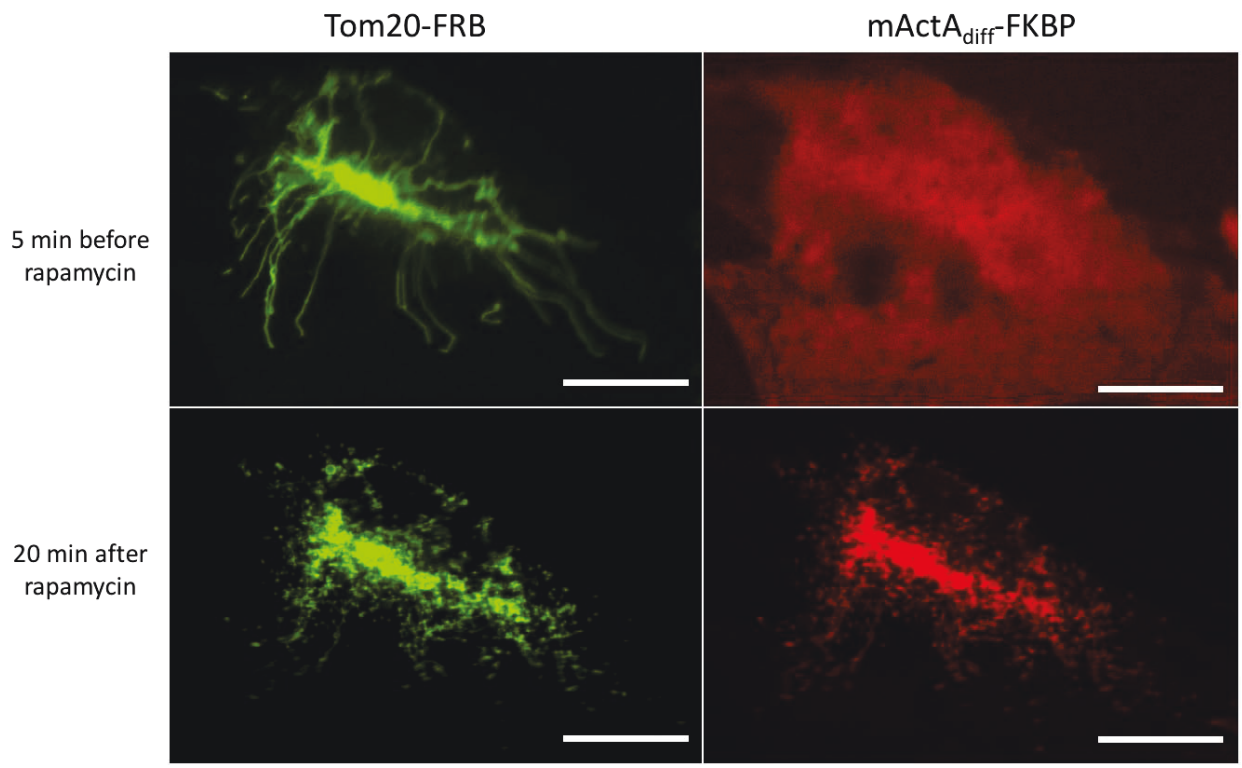


**Figure 3.9: mActA$_{diff}$ causes mitochondrial fragmentation in Drp1 KO MEFs.** Time lapse images of a representative Drp1 KO MEFs cells subjected to mActA$_{diff}$ fragmentation. After 20min, Drp1KO MEFs exhibits fragmentation.

# 3.2 Characterizing the Mitochondrial Fragments

However, these results do not prove that the mitochondria are truly fragmented by mActA$_{diff}$ and as a matter of fact, it could be a result of the tubular mitochondria going in and out of the focal plane. To determine whether there is discontinuity amongst the fragments, Fluorescence Recovery After Photobleaching (FRAP) was conducted (Fig 3.10(a) and (b)). As a control, we first bleached the tubular mitochondria and looked for any recovery (Fig 3.10(b)). Next in the same cell, we induced fragmentation of the mitochondria and again carried out FRAP on one of the fragments (Fig 3.10(b). The FRAP data was fitted with a first order model (Fig 3.11). The fitted model parameters, as shown in Table 3.1, showed a significant difference compared to the control. The control showed a halftime recovery of 0.126s, and the fragmented mitochondria showed a halftime

recovery of 0.233s. The mobile fraction was around 30% whereas for the control, it was around 60%. This suggests that there is not much mitochondrial content flowing in and out of the fragmented mitochondria implying structural discontinuity.

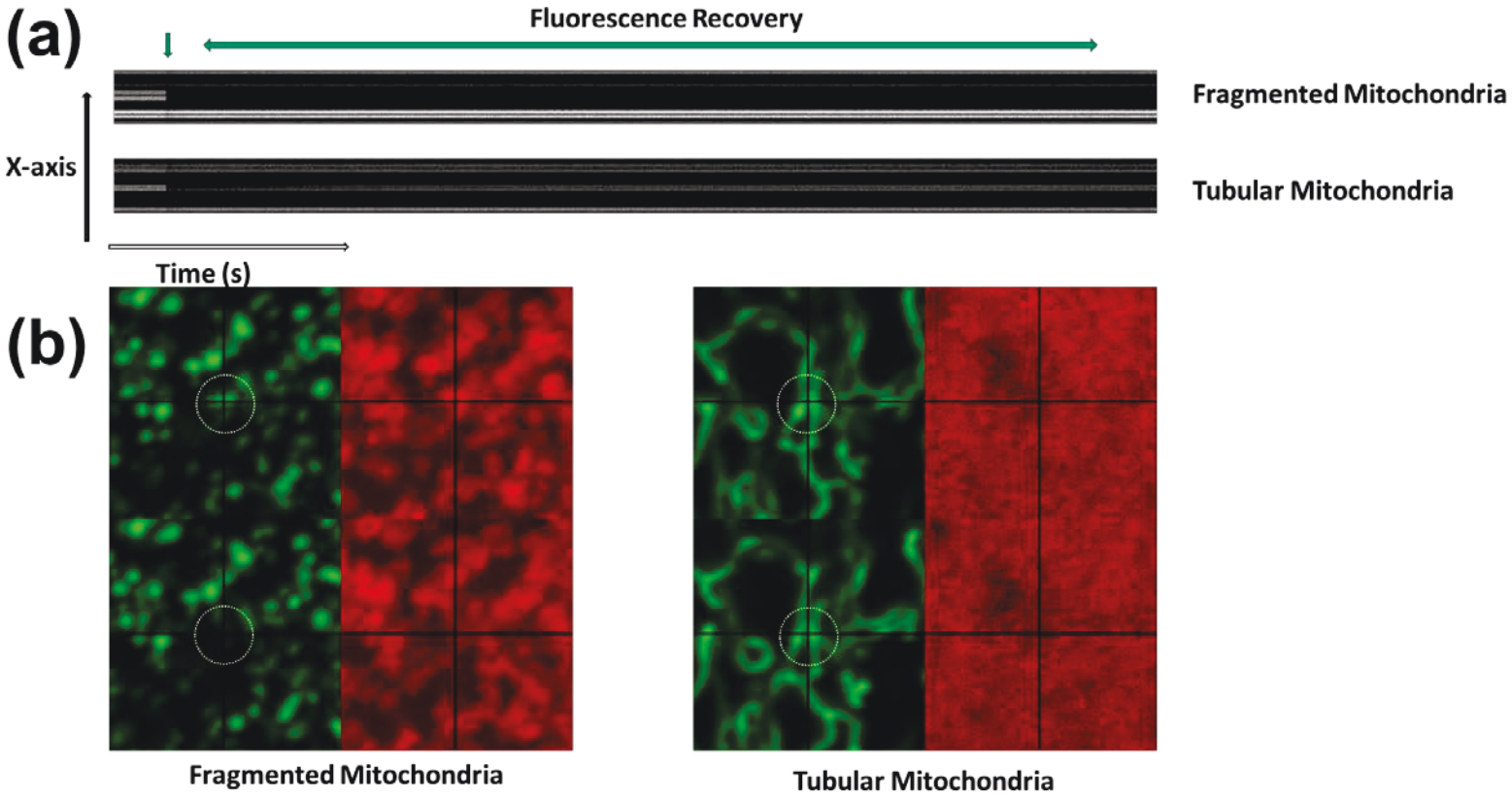


**Figure 3.10: mActA$_{diff}$ induced mitochondrial fragment did not recover its fluorescence after bleaching.** (a) Tubular mitochondria show fluorescence recovery after bleaching. (b) White circle indicates the region that was bleached. For mActA$_{diff}$ induced fragmented mitochondria the fluorescence did not recover.

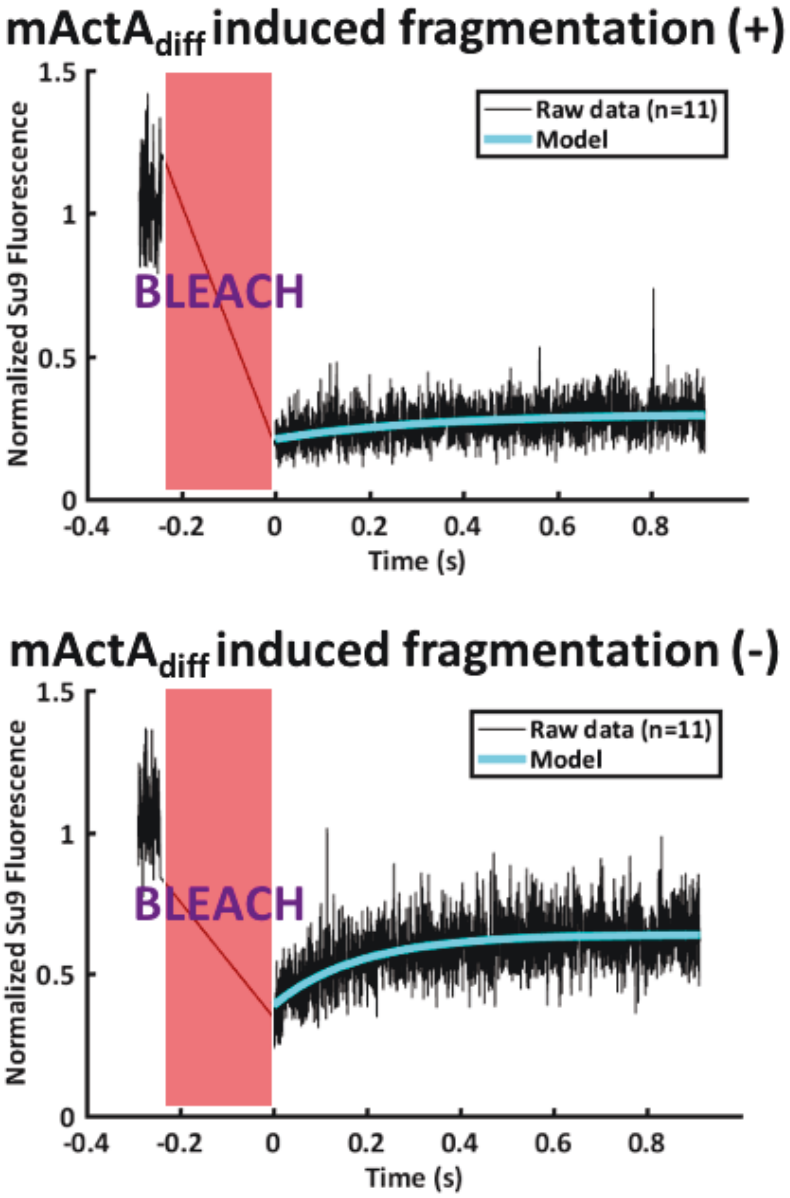


**Figure 3.11: mActA$_{diff}$ induced mitochondrial fragments are discontinuous in structure.** A quantitation of the fluorescent recovery before (bottom) and after (top) mActA$_{diff}$ inducd fragmentation.

| | TEST | Control | P-value |
|---|---|---|---|
| Foo | 0.2991 | 0.6396 | 0.0006 |
| A | 0.0894 | 0.2519 | 2.3186E-6 |
| $\tau$ | 0.3357 | 0.1820 | 0.1155 |
| $\tau 1/2$ | 0.232690 | 0.126153 | |

**Table 3.1: Model parameters that were used to fit the FRAP data.** A first order model was fitted to the FRAP data. Test: $mActA_{diff}$ induced fragmented mitochondria. Control: non-fragmented mitochondria. The difference between Foo and A gives the mobile fraction. $\tau 1/2$ is the half-recovery time. All parameters except $\tau$ showed significant difference relative to the control.

# Experiment 4

## 4.1 Short Term Effects on the Mitochondrial Function

Damaged mitochondria lose membrane potential, the ability to produce ATP, and affect ROS levels and calcium dynamics [55-58]. The malfunctioning mitochondria is recognized by the cell, and the impaired mitochondrial fragments undergo degradation through a process called mitophagy [55-58].

To test whether artificially inducing mitochondrial fragmentation changes membrane potential, we translocated $mActA_{diff}$ to the mitochondria and monitored the membrane potential using a dye called TMRE with its fluorescence as a readout. Few time points before the end of the imaging session, we added 10uM of CCCP as an internal positive control. Comparing the TMRE fluorescence values with the controls (DMSO: vehicle control, CCCP: positive control), we concluded there was nearly no change in membrane potential after fragmentation (Fig 3.12 (a)).

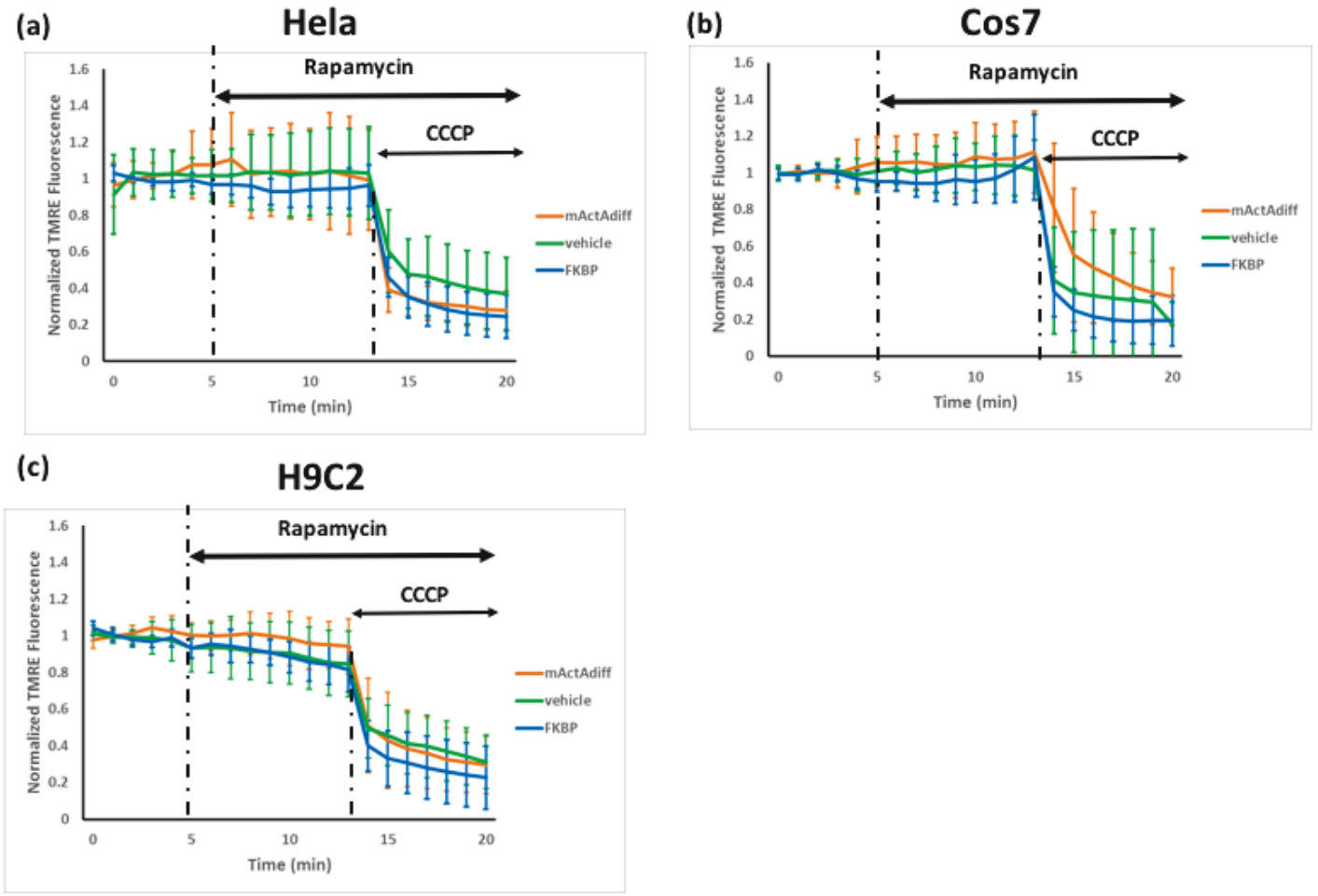


**Figure 3.12: mAct$A_{diff}$ does not change the membrane potential.** TMRE fluorescence was measured at the mitochondria and was normalized to the baseline. 10uM CCCP was added at 15min as an internal positive control. (a) Mitochondrial membrane potential of Hela cells overtime. (b) Mitochondrial membrane potential of Cos7 cells overtime. (c) Mitochondrial membrane potential of H9C2 cells overtime. 3 independent experiments were conducted.

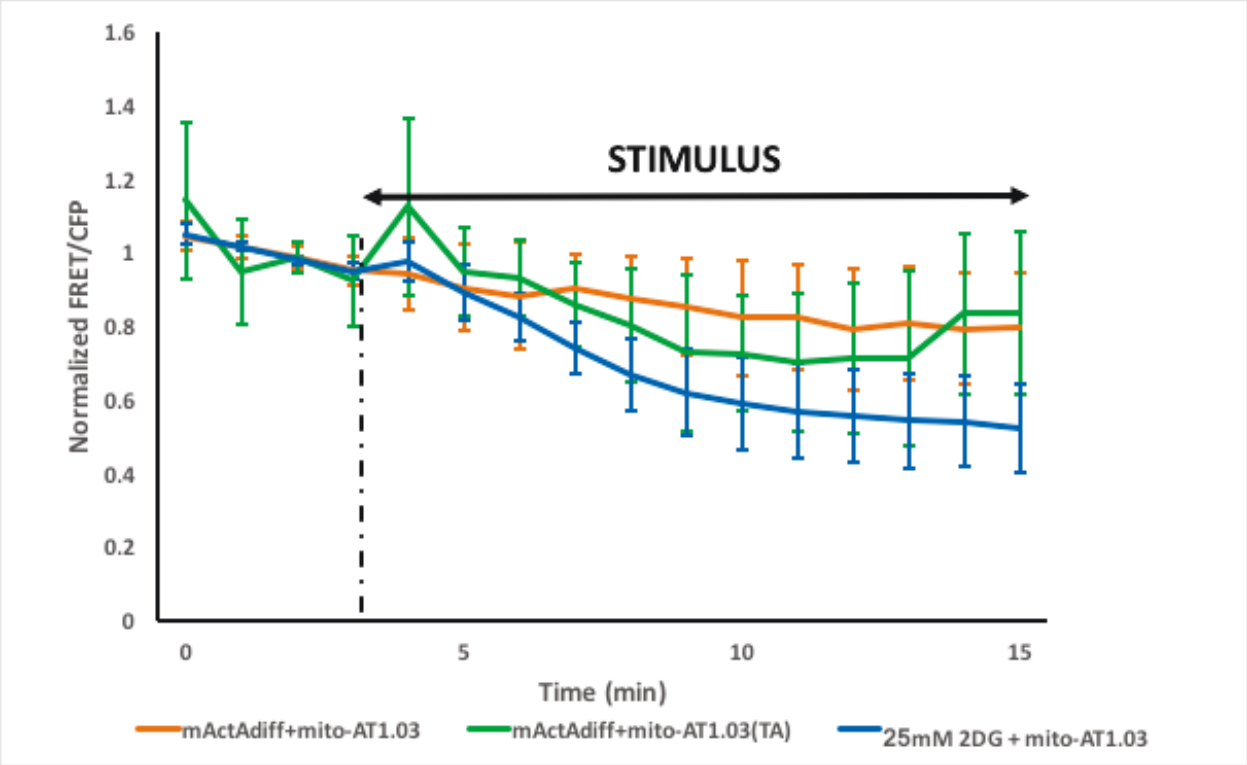


**Figure 3.13: No decreased ATP levels in mActA$_{diff}$ induced mitochondrial fragments.** The mitochondrial ATP level was measured by ATeam series [61]. Data shown is FRET/CFP normalized to the baseline. $P$=0.7758, $P$=6.8139x10$^{-7}$ compared to the negative control and positive control. 3 independent experiments were conducted.

We've also examined the short-term effects across different cell lines. In Cos7 cells, there was no significant change in membrane potential (Fig 3.12 (b)**)**. Likewise, we examined the effects on a cell line that is supposed to be more susceptible to mitochondrial integrity. We took a H9C2 cardiomyoblast cell line, which was isolated from ventricular tissue, and evaluated its functionality. Membrane potential of H9C2 cells did not change after fragmentation (Fig 3.12 (c)**).**

Next, using mito-AT1.03, an ATP FRET sensor, we tracked the ATP levels in the mitochondrial matrix overtime by measuring the FRET/CFP values. As shown in Fig 3.13, the FRET/CFP values dropped by a negligible amount, and there was no significant difference compared to the FRET/CFP values measured by mito-AT1.03 (R122K/R126K), the negative control.

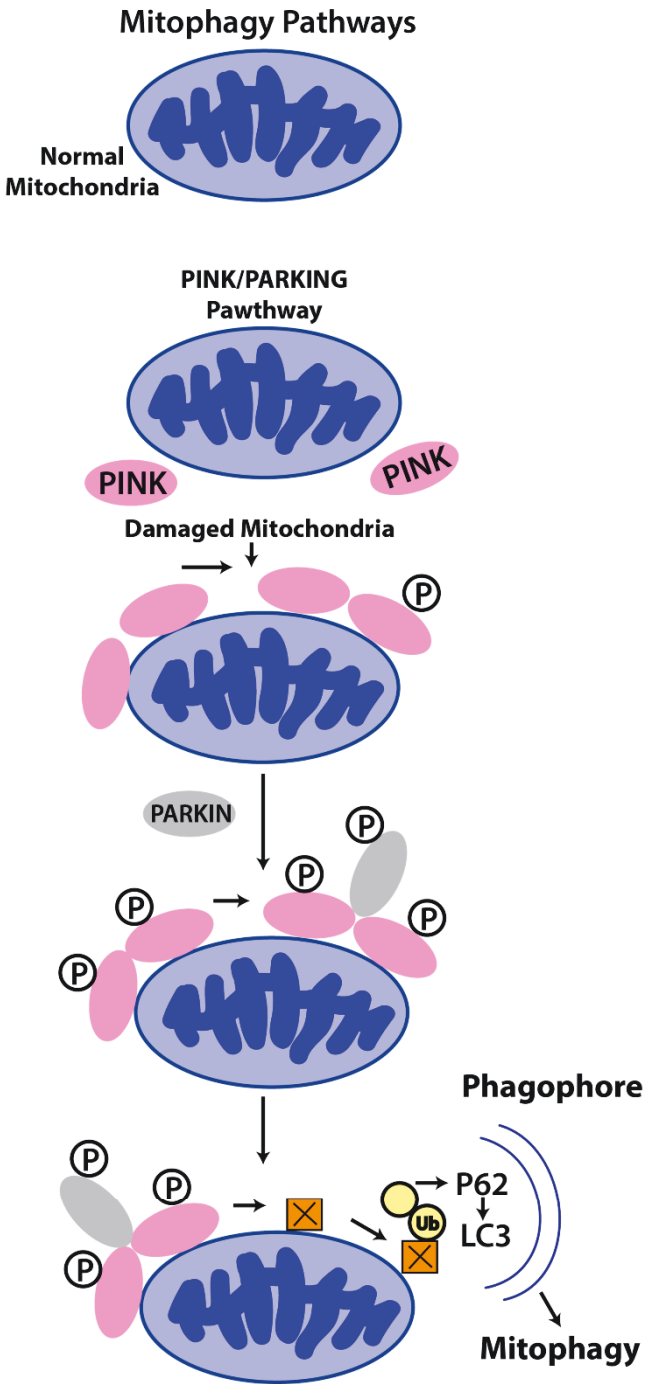


**Figure 3.14: An illustration of Parkin-dependent mitochondrial degradation pathway.** Parkin and LC3 are recruited to the damaged mitochondria for degradation.

## 4.2 Long Term Effects on the Mitochondrial Function

To see whether there were any long-term effects on the mitochondria, we looked for any indications of mitophagy. It has been reported that mitophagy goes through different stages recruiting different proteins along the way. Typically, an E4-ligase Parkin accumulates at the damaged mitochondria, and at a later stage, autophagy-specific adaptor protein LC3 starts to localize to the mitochondrial fragments which subsequently targets the mitochondria to autophagosomes [55-58] (Fig 3.14**)**. Therefore, we used these two proteins as markers for mitophagy. An end-point assay was carried out where the mitochondria was fragmented with $mActA_{diff}$ for 24hrs.

In Hela cells, less than 5% of the total area of mitochondria colocalized with Parkin (Fig 3.15) and for LC3, it was also less than 5% (Fig 3.16). This was statistically insignificant compared with the vehicle control ($P$=0.9178 and 0.8037, respectively). This was further confirmed with the fact that the membrane potential did not change 24hrs post fragmentation (Fig 3.17). We then tested whether the results could be reproduced in a different cell line.

In Cos7 cells, again less than 5% of the total area of mitochondria colocalized with Parkin and LC3 (Fig 3.15 and Fig 3.16). This was statistically insignificant compared with the vehicle control ($P$=0.9178 and 0.1932**)**. Interestingly, the membrane potential decreased after 24hrs (Fig 3.17).

Furthermore, in H9C2 cells, less than 5% of the total area of the mitochondria colocalized with Parkin and LC3. This was statistically insignificant compared with the vehicle control ($P$= 0.8442 and 0.0697). However, the membrane potential increased for H9C2 cells (Fig 3.17). For follow up experiments, it would be interesting if this translates to increase in ATP production rate.

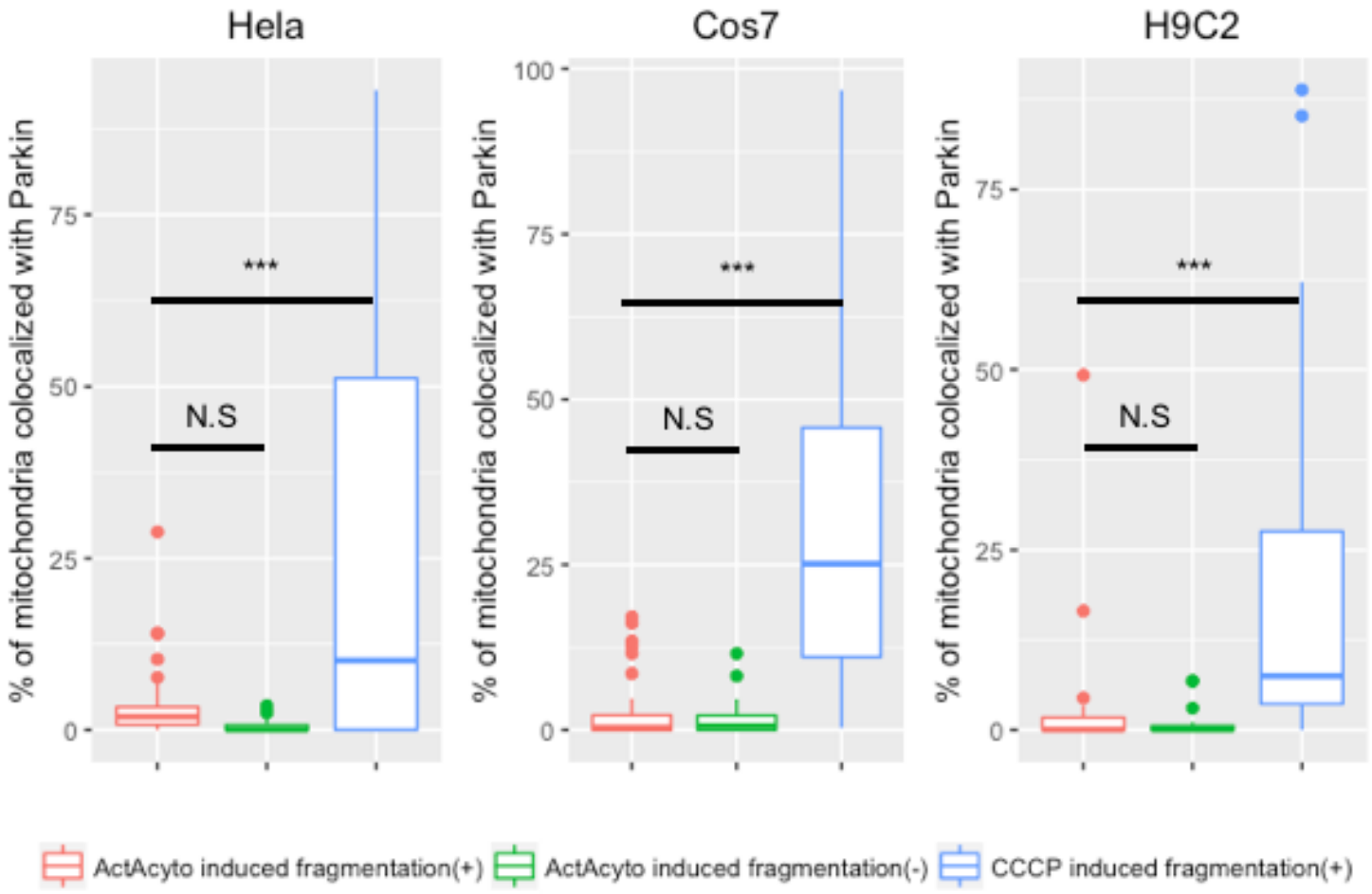


**Figure 3.15: Long term effects of $mActA_{diff}$ and Parkin co-localization.** Hela, Cos7, and H9C2 cells were subjected to fragmentation with either $mActA_{diff}$ or 10uM of CCCP for 24hrs. Data presents percentage area of mitochondria that colocalized with Parkin puncta. For Hela cells, $P$= 0.808 and $0.343x10^{-4}$. For Cos7 cells, $P$=0.9178 and $0.246x10^{-10}$. For H9C2 cells, $P$= 0.8442 and 0.001. (*N.S* indicates no statistical difference between the two groups. *$P$<0.1 **$P$<0.05, ***$P$<0.001.) 3 independent experiments were conducted.

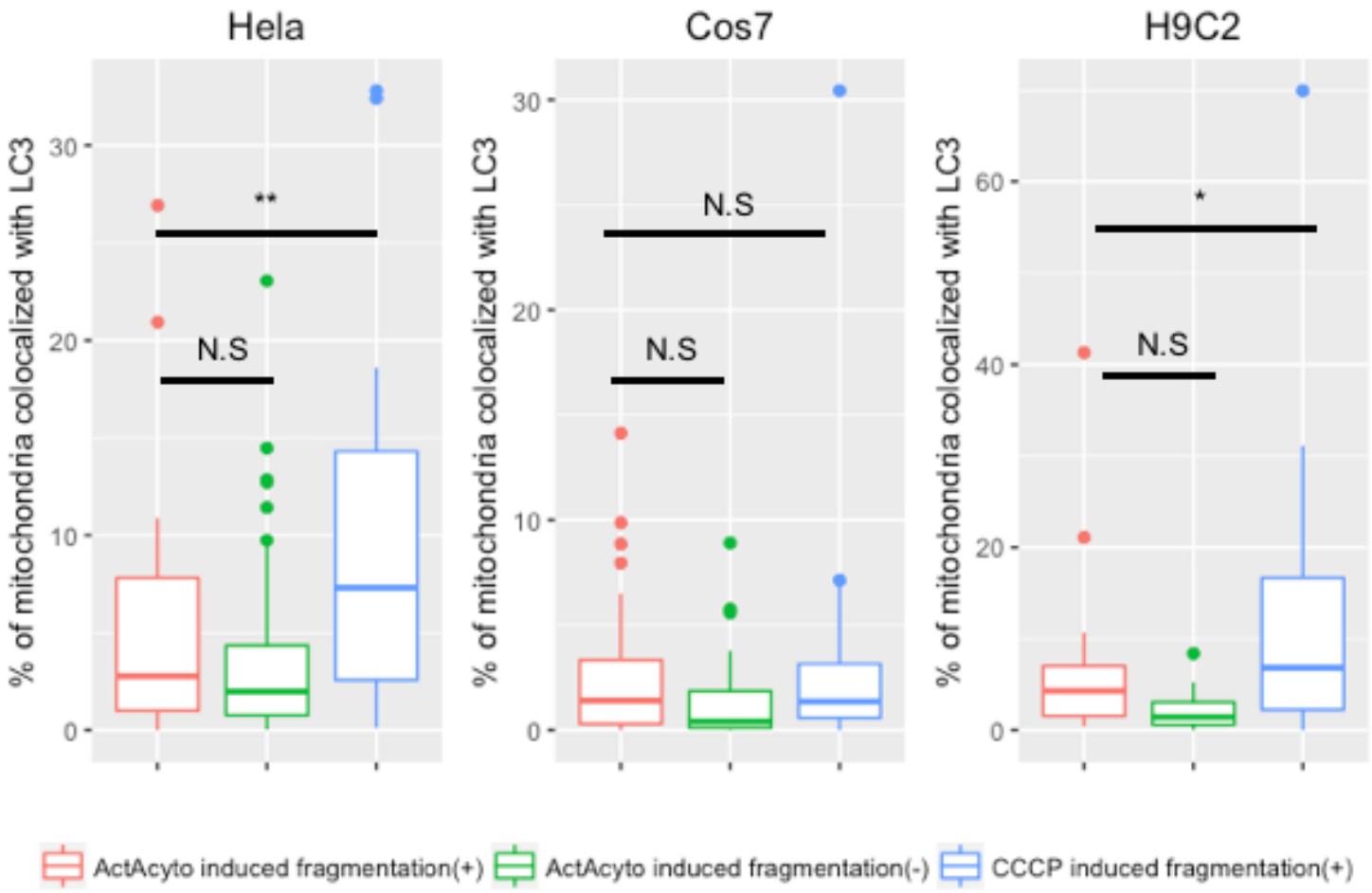


**Figure 3.16: Long term effects of mActA$_{diff}$ and LC3 co-localization.** Hela, Cos7, and H9C2 cells were subjected to fragmentation with either mActA$_{diff}$ or 10uM of CCCP for 24hrs. Data presents percentage area of mitochondria that colocalized with LC3 puncta. For Hela cells, $P$= 0.8037 and 0.0291. For Cos7 cells, $P$=0.1932 and 0.9936. For H9C2 cells, $P$= 0.1933 and 0.0697. (*N.S* indicates no statistical difference between the two groups. *$P$<0.1 **$P$<0.05, ***$P$<0.001.) 3 independent experiments were conducted.

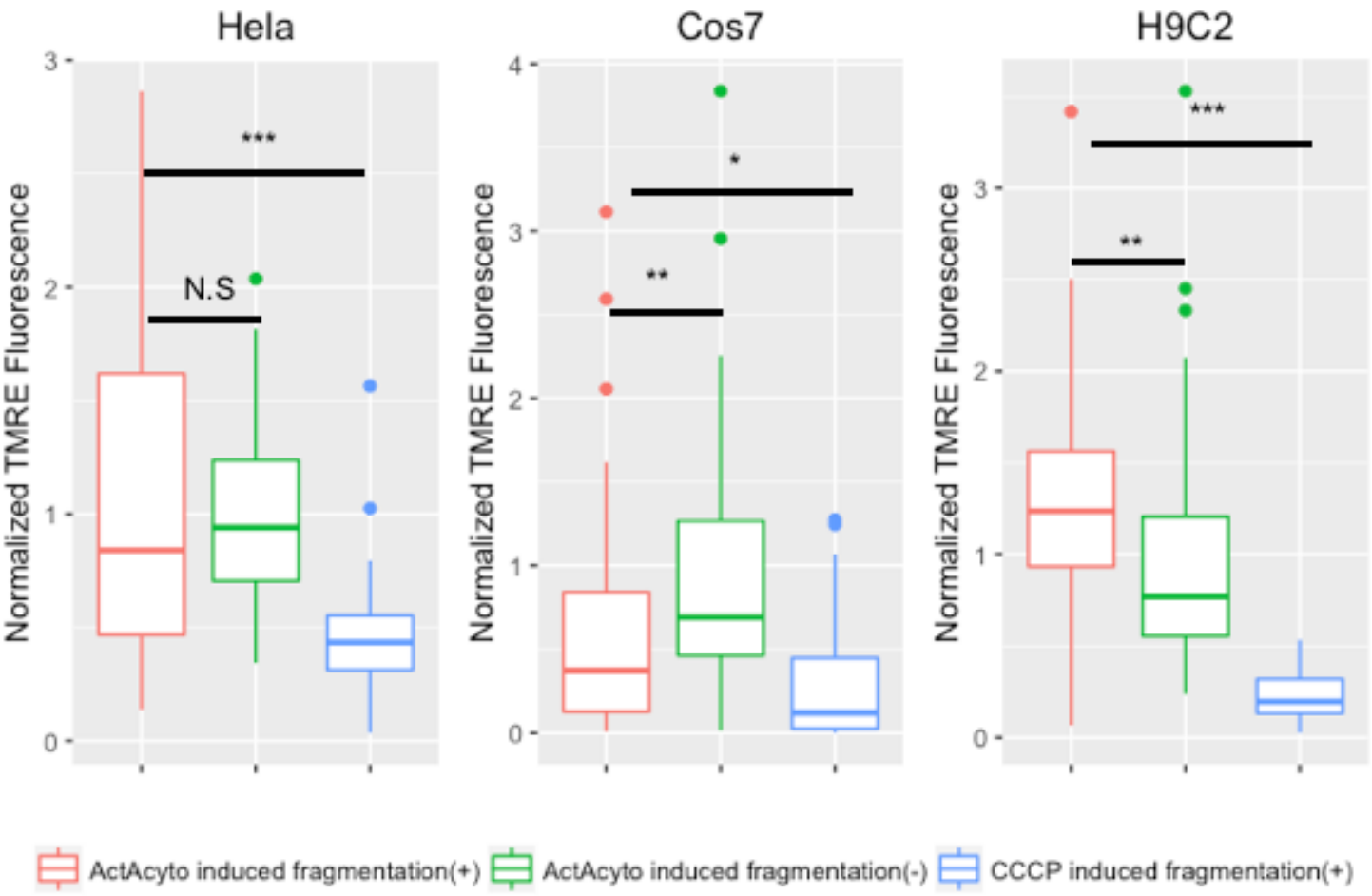


**Figure 3.17: Long term effects on mitochondrial membrane potential.** Hela, Cos7, and H9C2 cells were subjected to fragmentation with either $mActA_{diff}$ or 10uM of CCCP for 24hrs. Data presents percentage area of mitochondria that colocalized with Parkin puncta. For Hela cells, $P$= 0.6124 and $0.608x10^{-4}$. For Cos7 cells, $P$=0.0014 and 0.06. For H9C2 cells, $P$= 0.0142 and $0.4772x10^{-15}$. (*N.S* indicates no statistical difference between the two groups. *$P$<0.1 **$P$<0.05, ***$P$<0.001.) 3 independent experiments were conducted.

# Experiment 5

## 5.1 Reversible Manipulation of Mitochondrial Morphology

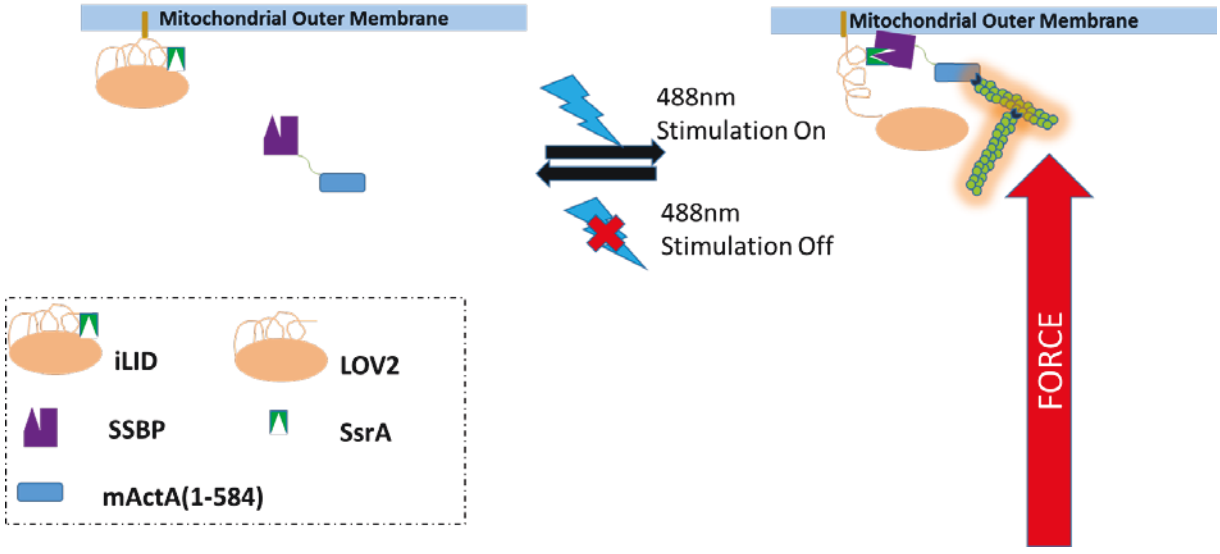


**Figure 3.18: Design of light-inducible mActA$_{diff}$.** Schematic of transcloated and untranslocated mActA$_{diff}$. Force generation occurs when mActA$_{diff}$ is recruited to the outer membrane of the mitochondria. This can be modulated with a 488nm laser.

One important shortcoming to our approach is that CID is nearly irreversible due to the low Kd between rapamycin and the dimerizers. This means that mActA$_{diff}$ is unlikely to dissociate

completely from the surface of the mitochondria and hence, persistently applying force. To tackle this issue, we resorted to light-inducible dimerization. Amongst the many light-inducible dimerization systems, we selected the light-induced dimer (iLID) system. iLID is composed of light-oxygen-voltage 2 (LOV2) domain from *Avena sativa* and a bacterial SsrA peptide. In the dark, SsrA is sterically inhibited and cannot bind to its partner, SspB. Upon illumination of blue light, LOV2 opens up allowing SsrA to bind to SspB [59]. Hoping to reversibly control force generation (Fig 3.18), we fused $mActA_{diff}$ to SspB and fused the mitochondrial outer membrane anchor protein, either MOA or TOM20, to iLID. After shining with 488nm laser, we saw an accumulation of $mActA_{diff}$ at the mitochondria which subsequently lead to mitochondrial fragmentation. As soon as we shut off the light, we saw $mActA_{diff}$ dissociate and the shape of the mitochondria returned to its initial tubular shape. We repetitively turned on and off the light and observed the mitochondria go from fragmentation to tubular forms (Fig 3.19 (a)). This was also reflected in F-actin signal increasing and decreasing at the surface of the mitochondria (Fig 3.19 (b), (c)) demonstrating that it is possible to control mitochondrial morphology.

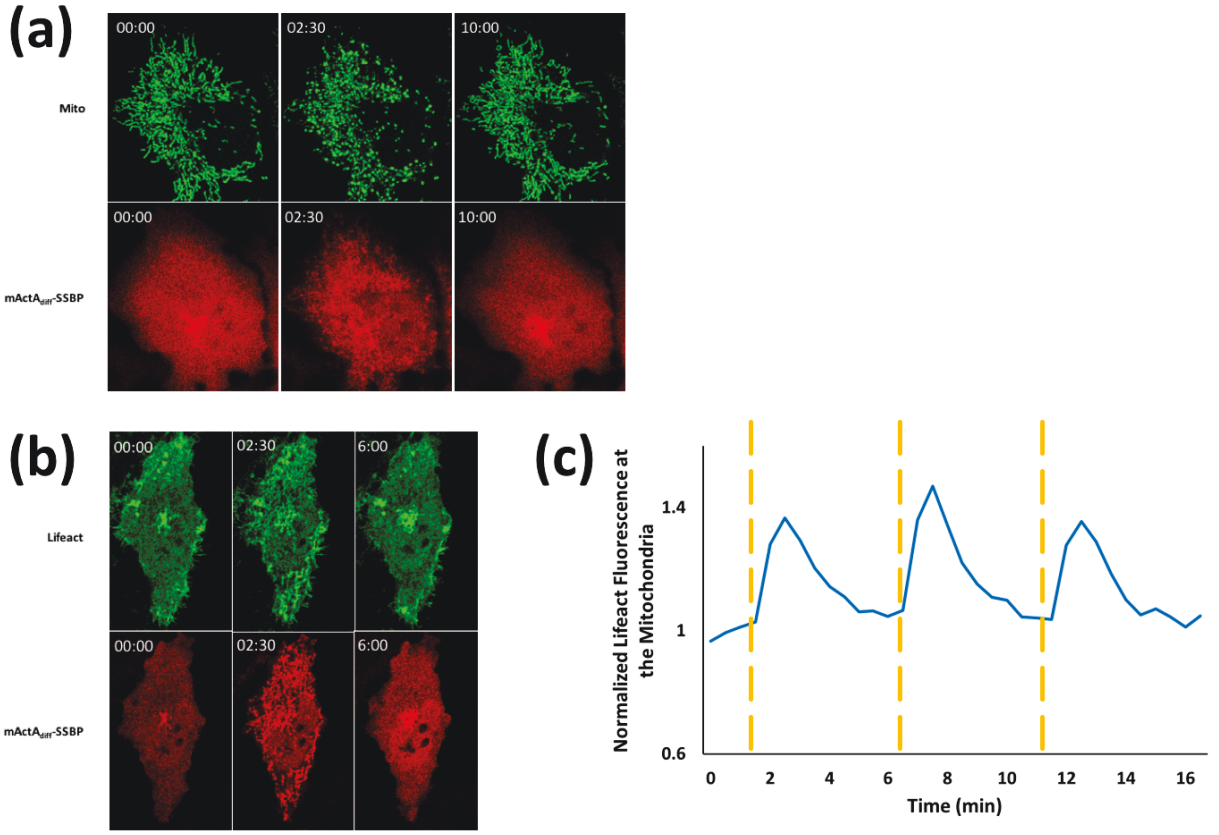


**Figure 3.19: mActA$_{diff}$ with iLID can be used to reversibly regulate mitochondrial morphology.** (a) Time lapse images of a representative Hela cell subjected to 488nm stimulation to initiate mActA$_{diff}$ based fragmentation. The morphology of the mitochondria returned to its initial shape approximately 8minutes after stimulation (b) Time lapse images of a representative Hela cell showing reversible control of actin polymerization at the mitochondria. (c) A quantitation of F-actin at the mitochondria. The yellow dashed lines indicate the point of stimulation.

## 5.2 Manipulating Other Organelles

Our next question was whether we could apply $mActA_{diff}$ to deform other organelles. To show the potential of $mActA_{diff}$ as a tool for other studying other various organelles, we targeted it to the endoplasmic reticulum.

To translocate $mActA_{diff}$ to the endoplasmic reticulum (ER), we used C-terminus tail of cytochrome b5 (Cb5) as our ER anchor and used KDEL as a separate marker for the ER. Approximately 10min after translocating $mActA_{diff}$ to the surface of the ER, we started to see deformation of the ER where it starts encroach into the nucleus. After approximately 1hr, the ER colocalized with the nucleus. Interestingly, as the ER invaded the nucleus, the nuclear localizing sequence (NLS) tagged fluorescent protein increased in the cytoplasm (Fig 3.20). To test the hypothesis whether nuclear cytoplasm shuttling was impaired, we repeated the experiment but instead had a nuclear exporting sequence (NES) tagged fluorescent protein. Interestingly, the NES signal increased in the nucleus as the ER deformed. This implies that there exists some mechanism that translates the structural impairment of ER to dysfunction in nucleus-cytoplasm protein shuttling.

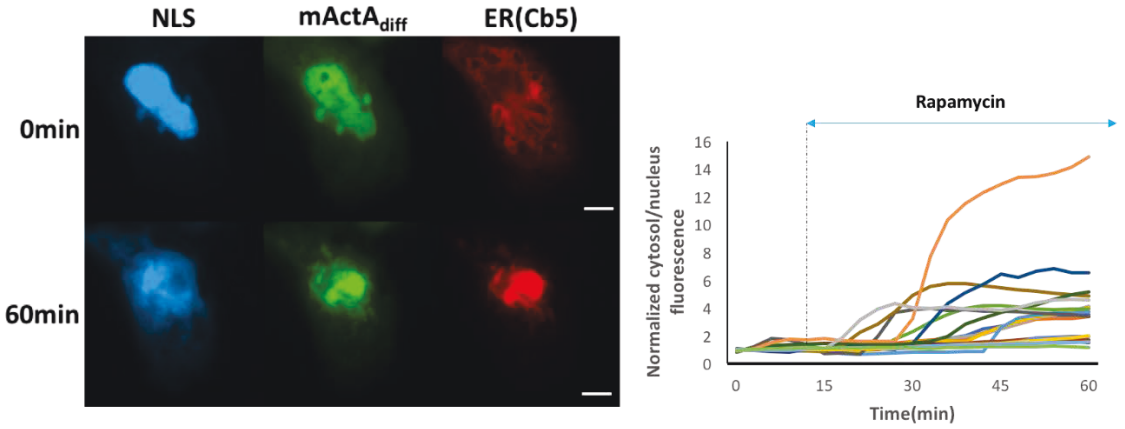


**Figure 3.20 NLS tagged fluorescent protein accumulates at the cytosol 60min after $mActA_{diff}$ recruitment.** (Left) Representative time lapse images of Hela cells undergoing ER deformation. (Right) Quantified NLS fluorescence at the cytosol divided by signal at the nucleus overtime.

# Conclusion

Deciphering the role of organelle morphology and its relevance to diseases has long been researcher's interest; however, limitation in existing tools to dissociate morphology and function has restricted our understanding of its true significance. In this study, we introduced a genetically encoded tool, $mActA_{diff}$, that could be used to directly change mitochondrial morphology, and potentially applied to other organelles as well.

We've shown that the fragmentation was actin dependent by inhibiting actin polymerization with Latrunculin A, involved Arp2/3 complex and was also independent of myosin II and Drp1. Furthermore, according to FRAP, each of mitochondrial fragments were discontinuous from each other. The fragmentation process could be similar to the process observed by Higgs's Group where they have shown that ER mediated actin polymerization recruits Drp1to constriction sites [60]. We don't know whether the differences we see in fragmentation across various cell lines is due to the variation in the physical property of the mitochondria or the disparities in expression level of mitochondrial fusion/fission proteins. Regardless, for all cases, we observed mitochondrial filament-like structures budding from the body of the mitochondria lead by an actin and ActA rich

head, subsequently leading to mitochondrial fragmentation. This could be a result of $mActA_{diff}$ pushing and creating a slight dent in the mitochondria redirects the force. In future experiments, it is important to elucidate whether $mActA_{diff}$ is fragmenting the mitochondria by pure force or through the help of endogenous fission machinery. It will be also interesting to see whether the inner membrane space or cristae capacity changes upon fragmentation.

We have shown that $mActA_{diff}$ induced mitochondrial fragmentation did not lead to any changes in membrane potential and ATP levels. Furthermore, there was no conclusive evidence of Parkin mediated mitophagy. Such results may suggest that the mitochondria were not damaged, but recalling how compelling the fragmentation was, it is hard to dismiss the possibility that there is perturbation. Another degradation process could be activated that is independent of Parkin. Further characterization is required such as evaluating the dynamic activity of the mitochondria or overall status of the cell. Do the mitochondria start to rely on a specific step of the electron transport chain? Are there any changes in import and export rate of certain molecules? Does the cell become more susceptible to drugs that otherwise would not be? These are some examples that could be perturbed by our system that is not captured in our assays.

Nevertheless, we have shown how effective our tool is to cause fragmentation. With the help of optogenetics, we believe this new tool will provide a new paradigm in studying organelle morphology, in particular mitochondrial morphology, by overcoming the limitations in the aforementioned methods to study mitochondrial moprhology.

# Materials/Methods

## Cell Culture and Transfection

All DNA constructs were transiently transfected using FugeneHD as a transfection reagent. Cells were plated on poly-D-lysine hydrobromide (Sigma)-coated cover glass. Cells were cultured in Dulbecco's modified Eagle's medium (DMEM;Gibco) supplemented with 10% fetal bovine serum and 1% penicillin/streptomycin at 37°C in 5% $CO_2$.

## Image Acquisition and Processing

24hr after transfection, cells were washed with Dublecco's Phosphate-Buffered Saline (DPBS) and fluorescent images of cells were taken using a. 63× objective (Plan-Apochromat, NA=1.4, Zeiss) mounted on an inverted Axiovert 135 TV microscope (Zeiss) and were captured by a QIClick charge-coupled device camera (QImaging). FRAP and light-induced dimerization experiments were conducted under Zeiss LSM780. Captured images were analyzed using an image processing software, Metamorph. All scale bars are 10um.

# Membrane Potential Analysis

Hela and H9C2 cells were stained with TMRE at a final concentration of 7nM whereas Cos7 cells were stained at a final concentration of 35nM. 10uM of CCCP was used to impair the membrane potential of the mitochondria or to induce mitophagy. 3 to 4 independent experiments were conducted.

# ATP Level Analysis

To measure the ATP levels in the mitochondrial matrix, an ATP FRET sensor, ATeam Series [61], was used. To lower the ATP levels, cells were cultured in either phenol red free DMEM with 25mM HEPES or the pyruvate free counterpart. 2-Deoxy-D-glucose (2-DG) was applied at a final concentration of 25mM to the cells to induce decrease in ATP level. 3 to 4 independent experiments were conducted.

# Actin and Myosin II Inhibition

Actin polymerization was inhibited with Latrunculin A at a final concentration 500nM. Myosin II was inhibited using blebbistatin at a final concentration of 50uM.

# Chemically-Induced-Dimerization and Light-Induced-Dimerization

Chemically-Induced-Dimerization was performed by adding rapamycin at a final concentration of 100nM to the prepared samples at the desired time point. Light-Induced-Dimerization was performed with Zeiss LSA780. Regions that were to be stimulated were selected using the built-in software and stimulated with the 488nm laser.

# Data Analysis

Either two-tailed student's t-test or one-way ANOVA following post hoc Scheffe's Method was used. All error bars are standard deviations.

# References


1. Heald, Rebecca, and Orna Cohen-Fix. "Morphology and function of membrane-bound organelles." *Current Opinion in Cell Biology* 26 (2014): 79-86.
2. Shibata, Yoko et al. Mechanisms determining the morphology of the peripheral ER. Cell (2010). Volume 143 , Issue 5 , 774 – 788.
3. Youle, R. J. et al. Mitochondrial Fission, Fusion, and Stress. Science. (2012). 337. 1062-1065.
4. Long , Q. et al. (2015) Modeling of mitochondrial donut formation. Biophys J.
5. Escobar-Heniques, M. et al . (2013). Mechanistic perspective of mitochondrial fusion: tubulation and fragmentation. Biochemica et Biophysica ActA. 1883. 162-175
6. Wai, T., Langer, T. (2016). Mitochondrial Dynamics and Metabolic Regulation. Trends in Endocrinology & Metabolism. 27. 105-117
7. Hoppins, S., Lackner, L., Nunnari, J. (2007). The machines that divide and fuse mitochondria. Annu Rev Biochem. 76. 751-80
8. Frezza, C., Cipolat, S., Brito, O. M., Micaroni, M., Beznoussenko, G. V., Rudka, T., Scorrano, L. (2006). OPA1 Controls Apoptotic Cristae Remodeling Independently from Mitochondrial Fusion. *Cell, 126*(1), 177-189.
9. Friedman, J.R. et al. (2014). Mitochondria form and function. Nature.
10. Ji, W., Hatch, A. L., Merrill, R. A., Strack, S., & Higgs, H. N. (2015). Actin filaments target the oligomeric maturation of the dynamin GTPase Drp1 to mitochondrial fission sites. *ELife, 4*.
11. Otera, H. et al. (2010). Mff is an essential factor for mitochondria recruitment of Drp1 during mitochondrial fission in mammalian cells. J. Cell Bio. 6, 1141-1158.
12. Hoitzing, Hanne, Iain G. Johnston, and Nick S. Jones. "What is the function of mitochondrial networks? A theoretical assessment of hypotheses and proposal for future research." *BioEssays* 37.6 (2015): 687-700.
13. Song, M. et al. Mitochondrial Fission and Fusion Factors Reciprocally Orchestrate Mitophagic Culling in Mouse Hearts and Cultured Fibroblasts. Cell Metabolism 21, 273-285.

14. Hamacher-Brady, Anne, and Nathan Ryan Brady. "Mitophagy programs: mechanisms and physiological implications of mitochondrial targeting by autophagy." *Cellular and Molecular Life Sciences* 73.4 (2015): 775-95.
15. Cassidy-Stone, Ann, Jerry E. Chipuk, Elena Ingerman, Cheng Song, Choong Yoo, Tomomi Kuwana, Mark J. Kurth, Jared T. Shaw, Jenny E. Hinshaw, Douglas R. Green, and Jodi Nunnari. "Chemical Inhibition of the Mitochondrial Division Dynamin Reveals Its Role in Bax/Bak-Dependent Mitochondrial Outer Membrane Permeabilization." *Developmental Cell* 14.2 (2008): 193-204.
16. Mishra, Prashant, and David C. Chan. "Mitochondrial dynamics and inheritance during cell division, development and disease." *Nature Reviews Molecular Cell Biology* 15.10 (2014): 634-46.
17. Knott, A. B. et al. Mitochondrial fragmentation in neurodegeneration. Nature Reviews Neuroscience. (2008).
18. Mishra, Prashant. "Interfaces between mitochondrial dynamics and disease." *Cell Calcium* 60.3 (2016): 190-98.
19. Wai, T., J. Garcia-Prieto, M. J. Baker, C. Merkwirth, P. Benit, P. Rustin, F. J. Ruperez, C. Barbas, B. Ibanez, and T. Langer. "Imbalanced OPA1 processing and mitochondrial fragmentation cause heart failure in mice." *Science* 350.6265 (2015):
20. Wisnovsky, Simon, Eric K. Lei, Sae Rin Jean, and Shana O. Kelley. "Mitochondrial Chemical Biology: New Probes Elucidate the Secrets of the Powerhouse of the Cell." *Cell Chemical Biology* 23.8 (2016): 917-27.
21. Graaf, Aniek O. De, Lambert P. Van Den Heuvel, Henry B.p.m. Dijkman, Ronney A. De Abreu, Kim U. Birkenkamp, Theo De Witte, Bert A. Van Der Reijden, Jan A.m. Smeitink, and Joop H. Jansen. "Bcl-2 prevents loss of mitochondria in CCCP-induced apoptosis." *Experimental Cell Research* 299.2 (2004): 533-40.
22. Gottlieb, E. et al. Mitochondrial membrane potential regulates matrix configuration and cytochrome c release during apoptosis. Cell Death Diff. (2003) 10(6): 709-7.
23. Lim, Maria L.r, Tetsuhiro Minamikawa, and Phillip Nagley. "The protonophore CCCP induces mitochondrial permeability transition without cytochromecrelease in human osteosarcoma cells." *FEBS Letters* 503.1 (2001): 69-74.
24. Ashrafi, Ghazaleh, Julia S. Schlehe, Matthew J. Lavoie, and Thomas L. Schwarz. "Mitophagy of damaged mitochondria occurs locally in distal neuronal axons and requires PINK1 and Parkin." *The Journal of Cell Biology* 206.5 (2014): 655-70.
25. Macia, E. et al. Dynasore, a cell-permeable inhibitor of dynamin. Developmental Cell 10,839-850.
26. Preta, G. et al. Dynasore- not just a dynamin inhibitor. Cell Communication and Signaling. (2015) 13:24. 1
27. Bordt, E. A. et al. The putative Drp1 inhibitor mdivi-1 is a reversible mitochondrial complex inhibitor that modulates reactive oxygen species. Dev. Cell (2017), 40(6), 583-594.
28. Cassidy-Stone, Ann, Jerry E. Chipuk, Elena Ingerman, Cheng Song, Choong Yoo, Tomomi Kuwana, Mark J. Kurth, Jared T. Shaw, Jenny E. Hinshaw, Douglas R. Green, and Jodi Nunnari. "Chemical Inhibition of the Mitochondrial Division Dynamin Reveals Its Role in Bax/Bak-Dependent Mitochondrial Outer Membrane Permeabilization." *Developmental Cell* 14.2 (2008): 193-204.

29. Lackner, L. L. et al. Small Molecule Inhibitors of Mitochondrial Division: Tools that Translate Basic Biological Research into Medicine. Chemistry and Biology (2010).
30. Logan, Angela, and Michael P. Murphy. "Using chemical biology to assess and modulate mitochondria: progress and challenges." *Interface Focus* 7.2 (2017)
31. Eisner, Veronica, Ryan Cupo, Csordas Gyorgy, Lan Cheng, Walter Koch, and Gyorgy Hajnoczky. "Mitochondrial Dynamics in Neonatal and Adult Cardiomyocytes." *Biophysical Journal* 106.2 (2014)
32. Alirol, E., and J. C. Martinou. "Mitochondria and cancer: is there a morphological connection?" *Oncogene* 25.34 (2006): 4706-716.
33. McCarron, J. G., et al. From Structure to Function: Mitochondrial Morphology, Motion and Shaping in Vascular Smooth Muscle. J Vasc Res. (2013). 357-371.
34. Mooren, Olivia L., Brian J. Galletta, and John A. Cooper. "Roles for Actin Assembly in Endocytosis." *Annual Review of Biochemistry* 81.1 (2012): 661-86.
35. Akhshi, Tara Kafiyeh, Denise Wernike, and Alisa Piekny. "Microtubules and actin crosstalk in cell migration and division." *Cytoskeleton* 71.1 (2013): 1-23.
36. Depina, Ana S., and George M. Langford. "Vesicle transport: The role of actin filaments and myosin motors." *Microscopy Research and Technique* 47.2 (1999): 93-106.
37. Pelham, Robert J., and Fred Chang. "Actin dynamics in the contractile ring during cytokinesis in fission yeast." *Nature* 419.6902 (2002): 82-86.
38. Goode, Bruce L., and Michael J. Eck. "Mechanism and Function of Formins in the Control of Actin Assembly." *Annual Review of Biochemistry* 76.1 (2007): 593-627.
39. Schuldt, Alison. "Spire: a new nucleator for actin." *Nature Cell Biology* 7.2 (2005): 107
40. Goley, Erin D., and Matthew D. Welch. "The ARP2/3 complex: an actin nucleator comes of age." *Nature Reviews Molecular Cell Biology* 7.10 (2006): 713-26.
41. Zalevsky, J., I. Grigorova, and R. D. Mullins. "Activation of the Arp2/3 Complex by the Listeria ActA Protein: ActA BINDS TWO ACTIN MONOMERS AND THREE SUBUNITS OF THE Arp2/3 COMPLEX." *Journal of Biological Chemistry* 276.5 (2000): 3468-475.
42. Lambrechts, Anja, Kris Gevaert, Pascale Cossart, Joël Vandekerckhove, and Marleen Van Troys. "Listeria comet tails: the actin-based motility machinery at work." *Trends in Cell Biology* 18.5 (2008): 220-27.
43. Chong, Ryan, Rachel Swiss, Gabriel Briones, Kathryn L. Stone, Erol E. Gulcicek, and Hervé Agaisse. "Regulatory Mimicry in Listeria monocytogenes Actin-Based Motility." *Cell Host & Microbe* 6.3 (2009): 268-78.
44. Rafelski, Susanne M., and Julie A. Theriot. "Bacterial Shape and ActA Distribution Affect Initiation of Listeria monocytogenes Actin-Based Motility." *Biophysical Journal* 89.3 (2005): 2146-158.
45. Lacayo, C. I., P. A. G. Soneral, J. Zhu, M. A. Tsuchida, M. J. Footer, F. S. Soo, Y. Lu, Y. Xia, A. Mogilner, and J. A. Theriot. "Choosing orientation: influence of cargo geometry and ActA polarization on actin comet tails." *Molecular Biology of the Cell* 23.4 (2012): 614-29.
46. Lauer, Peter, Julie A. Theriot, Justin Skoble, Matthew D. Welch, and Daniel A. Portnoy. "Systematic mutational analysis of the amino-terminal domain of the Listeria monocytogenes ActA protein reveals novel functions in actin-based motility." *Molecular Microbiology* 42.5 (2002): 1163-177.

47. Smith, G. A. "The tandem repeat domain in the Listeria monocytogenes ActA protein controls the rate of actin-based motility, the percentage of moving bacteria, and the localization of vasodilator-stimulated phosphoprotein and profilin." *The Journal of Cell Biology* 135.3 (1996): 647-60.
48. Lasa, I. "Identification of two regions in the N-terminal domain of ActA involved in the actin comet tail formation by Listeria monocytogenes." *The EMBO Journal*16.7 (1997): 1531-540.
49. Rafelski, Susanne M., Jonathan B. Alberts, and Garrett M. Odell. "An Experimental and Computational Study of the Effect of ActA Polarity on the Speed of Listeria monocytogenes Actin-based Motility." *PLoS Computational Biology* 5.7 (2009).
50. Soo, Frederick S., and Julie A. Theriot. "Large-Scale Quantitative Analysis of Sources of Variation in the Actin Polymerization-Based Movement of Listeria monocytogenes." *Biophysical Journal* 89.1 (2005): 703-23.
51. Merz, Alexey J., and Henry N. Higgs. "Listeria Motility: Biophysics Pushes Things Forward." *Current Biology* 13.8 (2003)
52. Upadhyaya, A., J. R. Chabot, A. Andreeva, A. Samadani, and A. Van Oudenaarden. "Probing polymerization forces by using actin-propelled lipid vesicles." *Proceedings of the National Academy of Sciences* 100.8 (2003): 4521-526.
53. Smith, Gregory A., and Daniel A. Portnoy. "How the Listeria monocytogenes ActA protein converts actin polymerization into a motile force." *Trends in Microbiology* 5.7 (1997): 272-76.
54. Derose, Robert, Takafumi Miyamoto, and Takanari Inoue. "Manipulating signaling at will: chemically-inducible dimerization (CID) techniques resolve problems in cell biology." *Pflügers Archiv - European Journal of Physiology* 465.3 (2013): 409-17.
55. Dolman, Nick J., Kevin M. Chambers, Bhaskar Mandavilli, Robert H. Batchelor, and Michael S. Janes. "Tools and techniques to measure mitophagy using fluorescence microscopy." *Autophagy* 9.11 (2013): 1653-662.
56. Cai, Qian, Hesham Mostafa Zakaria, Anthony Simone, and Zu-Hang Sheng. "Spatial Parkin Translocation and Degradation of Damaged Mitochondria via Mitophagy in Live Cortical Neurons." *Current Biology* 22.6 (2012): 545-52.
57. Nguyen, Thanh N., Benjamin S. Padman, and Michael Lazarou. "Deciphering the Molecular Signals of PINK1/Parkin Mitophagy." *Trends in Cell Biology* 26.10 (2016): 733-44.
58. Narendra, Derek, Atsushi Tanaka, Der-Fen Suen, and Richard J. Youle. "Parkin is recruited selectively to impaired mitochondria and promotes their autophagy." *The Journal of Cell Biology* 183.5 (2008): 795-803.
59. Guntas, Gurkan, Ryan A. Hallett, Seth P. Zimmerman, Tishan Williams, Hayretin Yumerefendi, James E. Bear, and Brian Kuhlman. "Engineering an improved light-induced dimer (iLID) for controlling the localization and activity of signaling proteins." *Proceedings of the National Academy of Sciences* 112.1 (2014): 112-17.
60. Ji, Wei-Ke, Anna L. Hatch, Ronald A. Merrill, Stefan Strack, and Henry N. Higgs. "Actin filaments target the oligomeric maturation of the dynamin GTPase Drp1 to mitochondrial fission sites." *ELife* 4 (2015)
61. Imamura, H., K. P. Huynh Nhat, H. Togawa, K. Saito, R. Iino, Y. Kato-Yamada, T. Nagai, and H. Noji. "Visualization of ATP levels inside single living cells with fluorescence

resonance energy transfer-based genetically encoded indicators." *Proceedings of the National Academy of Sciences* 106.37 (2009): 15651-5656.

# Vita

Elmer Rho was born in Washington on January 11, 1993. He attended Johns Hopkins University from 2011 to 2015 and received a Bachelor of Arts with honors in Biophysics, Applied Math/Statistics, and Physics in 2015. He worked toward a Master of Engineering in Biomedical Engineering at Johns Hopkins University in the Fall of 2015. During his career, he has been involved in different projects resulting in various papers and received a NSF GRFP Honorable Mention. He will be pursuing a PhD in Systems Biology at Harvard University beginning the Fall of 2017.